University of Natural Resources and Life Sciences, Vienna

Purification of rh-TNF-α by chromatographic methods

Markus Christian Berg, B. Sc.

Master Thesis

in partial fulfillment of the requirements for the degree of

Diplom-Ingenieur

Department of Biotechnology

University of Natural Resources and Life Science, Vienna

Department Head: Univ.Prof.Dipl.-Ing. Dr. rer.nat Reingard Grabherr

Supervisor: Assoc. Prof. Dipl.-Ing. Dr. Rainer Hahn

Co-Supervisor: Dipl.-Ing. Dr. Astrid Dürauer

Eidesstattliche Erklärung

Ich erkläre eidesstattlich, dass ich die Arbeit selbständig angefertigt, keine anderen als die angegebenen Hilfsmittel benutzt und alle aus ungedruckten Quellen, gedruckter Literatur oder aus dem Internet im Wortlaut oder im wesentlichen Inhalt übernommenen Formulierungen und Konzepte gemäß den Richtlinien wissenschaftlicher Arbeiten zitiert, durch Fußnoten gekennzeichnet bzw. mit genauer Quellenangabe kenntlich gemacht habe.

Wien,_____ _____

Datum Unterschrift

Acknowledgement

I would like to express my deepest appreciation to my supervisors Rainer Hahn as well as Astrid Dürauer for their help during my master thesis and of course for their valuable input. Furthermore, I want to thank my working group colleagues for their support.

Most importantly, I want to thank my family and everyone else who supported me morally over the period of my studies.

Zusammenfassung

Tumor Nekrose Faktor Alpha (TNF-α) ist ein Zytokin, das für therapeutische Zwecke Verwendung findet. TNF-α wird rekombinant in dem bakteriellen Wirtsorganismus Escherichia coli hergestellt. In seiner physiologisch wirksamen Form liegt das Protein als Trimer vor. Ziel dieser Arbeit war die Entwicklung eines Aufarbeitungsprozesses für aktiven TNF-α. Es wurde eine 2-stufige chromatographische Aufreinigung, basierend auf einem Anionentauscher, gefolgt von einem Kationentauscher, etabliert. Mit diesem 2-stufigen Prozess, und dem Einsatz einer Stufenelution mit Natriumchlorid, konnte unter optimierten Bedingungen eine Ausbeute von 60% an aktivem TNF-α erzielt werden. Analytische Untersuchungen zeigten allerdings eine Reinheit von nur 20%. Die Implementation eines linearen Salzgradienten zur Elution des Produktes im 2. Schritt ermöglichte die Gewinnung von trimeren TNF-α mit einer Reinheit > 95%. Die Gesamtausbeute der Aufreinigung lag in diesem Fall allerdings nur bei 5%, was daran lag, dass ein Großteil des TNF-α in Assoziation mit Wirtszellproteinen eluierte. Als grundlegende Limitierung des Prozesses stellte sich die geringe Bindungskapazität der beiden Ionentauschern heraus. Detaillierte Analysen des Ausgangsmaterials zeigten, dass ein überwiegender Teil des von der Zelle produzierten TNF-α als Aggregat von TNF-α - Monomeren mit dem äußeren Membranprotein F (ompF) und dem Phagen-Shock-Protein A vorlag. Es konnte gezeigt werden, dass dieses Aggregat für die geringe Bindungskapazität des trimeren Produktes verantwortlich ist. Eine Verbesserung der Produktivität dieses Prozesses könnte daher durch die Destabilisierung dieser Aggregate erzielt werden. Hitzebehandlung bei 60°C oder Inkubation mit 2 M Harnstoff haben sich in ersten Versuchen als zielführend erwiesen.

Abstract

Tumor necrosis factor alpha (TNF-α) is a cytokine that has found broad therapeutic application. The protein is produced recombinantly in the host organism Escherichia coli. In its physiological active form TNF-α exists as a trimer linked by non-covalent bonds. The goal of this work was to establish a purification process to obtain active TNF-α. A two-stage chromatographic process based on an anion exchanger, followed by a cation-exchanger was developed. Using a step elution with NaCl in both steps a yield of approximately 60% of trimeric TNF-α was obtained under optimized conditions. The analysis of the product revealed a purity of only 20%. Implementation of a linear NaCl gradient for elution from the cation exchanger yielded TNF-α with a purity of > 95%. However, the overall process yield was only 5%. The reason for this very low yield of highly pure TNF-α was the fact that the major fraction of the protein eluted in association with host cell proteins. As another crucial limitation of the purification process the low binding capacity of both ion exchangers was identified. Detailed analysis of the primary cell homogenate showed that the majority of TNF-α produced by the cells was expressed in form of an aggregate consisting of monomeric TNF-α and two other host proteins, the outer membrane protein F (ompF) and the phage shock protein A. Binding studies with the anion exchanger showed that the presence of these aggregates significantly reduced the binding capacity for the trimeric TNF-α. Higher productivity could therefore be achieved by destabilization or even breakage of this aggregate. Preliminary experiments identified heat treatment at 60°C and incubation in presence of 2 M urea as suitable approaches for this purpose.

Table of contents

1. Introduction

Fast growth characteristics, facile scale-up as well as other beneficial properties support the use of *Escherichia coli* (E. coli) as the microbiological factory of choice for the production of recombinant proteins. Nowadays, approximately 30 percent of all approved therapeutically proteins are still produced in the gram negative bacteria [1]. Cytoplasmic and periplasmic expression enables high production titers of protein of interest. Moreover, periplasmic production offers some major advantages over cytoplasmic expression such as reduced proteolytic degradation and improved protein folding [2]. Besides the wide range of advantages regarding the use of E. coli, some properties could possibly lead to difficulties during the whole production and purification cycle. Due to the molecular basis of E. coli a lot of intracellular processes have to take place in parallel and hence sometimes lead to impreciseness. An overproduction of a specific protein, for instance, could result in the formation of misfolded aggregates, also called inclusion bodies (IB). These IBs are more or less an accumulation of proteins that exhibit incorrect disulfide bond formation or in general an insufficient and incorrect folding. The reason for this phenomenon is the overburden of factors responsible for proper folding [3,4]. Despite E. coli is one of the most stable production systems inadvertent conditions could influences accurate protein expression in a significant way.

One example of a therapeutic protein produced in E. coli is the tumor necrosis factor-alpha (TNF-α). The Purification of this pro-inflammatory cytokine by different chromatographic methods has been described in several published articles. They mostly differ in using various unit operations. Although Escherichia coli is a well described and studied organism, protein purification can as well sometimes lead to unexpected results where their origin is not clarified.

1.1. Tumor necrosis factor-alpha (TNF-α)

1.1.1 Classification of Cytokines

Differentiation and communication between cells are, amongst other functions, effected by secreting small proteins called cytokines. These pleiotropic signal molecules can act directly on cells of which they originate as well as on adjacent cells [5].

Basically, cytokines can be divided into six functional classes which differ in their biological effect:

interleukins (IL) – stimulation of haematopoiesis (blood cell formation)
chemokines - promotion of angiogenesis (formation and growth of blood vessels)
interferons (INF) – induction of antiviral immunity
tumor necrosis factor (TNF) – cell survival and death
colony stimulating factors – generation and maturation of macrophages
transforming growth factor-beta (TGF-β) – triggers production of extracellular matrix[6,7,8,9]

Furthermore, the tumor necrosis factor superfamily include the subspecies TNF-α, which is mainly produced in activated macrophages and TNF-beta, produced in cytotoxic T-lymphocytes [10].

In 1985, 20 years after the first documentation of TNF related tumor regression, a cytokines research group in Texas, USA, managed to distinguish between the two major types of the TNF superfamily as well as cloning their genes. Basically, TNF-α and TNF-β show an amino acid homology of approximately 50% and thereof differ in size and other biological properties. Results of some experiments on the cancer related disease cachexia, where TNF-α plays a key role, led to its sobriquet "cachectin" [11,12]. In vivo, TNF-α is primarily produced as a 26-kDa large precursor protein, composed of 233 amino acids, that has to undergo a proteolytic cleavage process to fully mature: the pro-TNF is a transmembrane protein, where its N-terminus is located on the inside of the cell, the cytoplasm, and its C-terminus can be found in the extracellular domain [13,14]. After forming a non-covalently linked homotrimer, consisting of three transmembrane pro-TNF monomers, a TNF-α converting enzyme (TACE) cleaves each monomer between Ala76 and Val77 on the extracellular side. This trimming results in mature 17-kDa (157 amino acids long) soluble TNF-α monomers, which are still assembled

to a trimeric form. Finally, the remaining transmembrane/intracellular amino acid chains are enzymatically processed and partly used as mediator for cytokine production [14,15].
It is important to mention that both types of trimers, the transmembrane (tmTNF-α) as well as the soluble form (sTNF-α), are active regarding the ability to bind receptors. A schematic drawing of the trimming process and receptor binding is displayed in Figure 1.

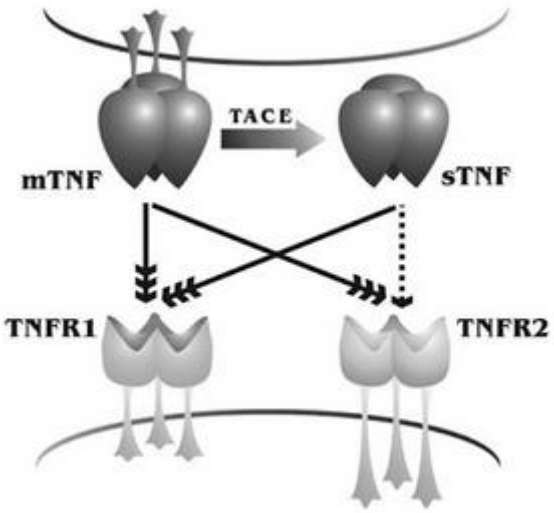

Figure 1: Trimming by TACE and binding process of tmTNF-α and sTNF-α to TNF-receptor 1 (TNFR1) and TNF-receptor 2 (TNFR2) [16].

The TNF related receptors (TNFR1 and TNFR2) have to form trimers as well to allow proper binding and further signal transmission. The interaction between sTNF and TNFR2 is less affine, signalized by the dotted arrow [9].

1.1.2. Properties of sTNF-α

According to RCSB Protein Data Bank [17] the primary structure (amino acids sequence) of each monomer is composed as follows:

VRSSSRTPSD KPVAHVVANP QAEGQLQWLN RRANALLANG
VELRDNQLVV PSEGLYLIYS QVLFKGQG**C**P STHVLLTHTI
SRIAVSYQTK VNLLSAIKSP **C**QRETPEGAE AKPWYEPIYL
GGVFQLEKGD RLSAEINRPD YLDFAESGQV YFGIIAL

Three syngeneic processed TNF monomers, consisting of 157 amino acids, form the active soluble TNF-α trimer (molecular weight of 52-kDa). The wedge-like structure of each subunit is composed of antiparallel-β sheets and corresponds to the viral capsid jelly roll motif. This described motif is visualized in Figure 2. The exposed N-terminus is not part of the core region of the protein, it is embedded in the base and not essential for trimer interactions as well as biological activities. The lightening flash indicates the disulfide bond between the two cysteine residues, which are as well highlighted in the primary structure.

X-ray crystallography studies have shown that the mature trimeric protein exhibits a conical structure with 5.5 nm length and 5.0 nm breadth [13,18].

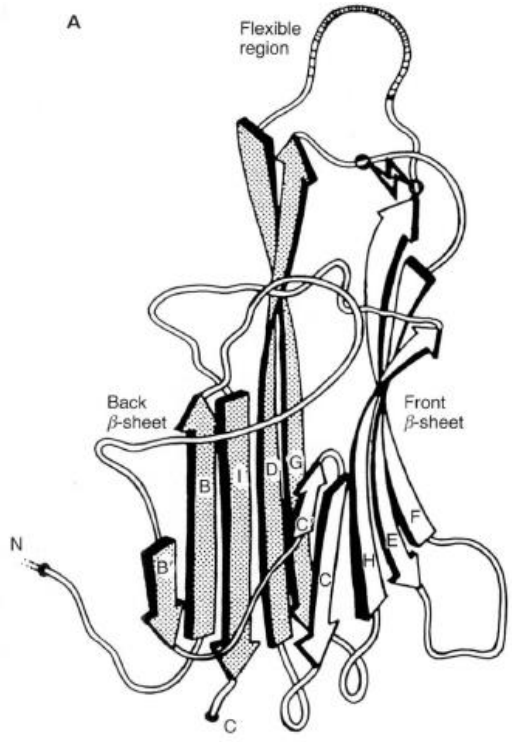

Figure 2: Structure of TNF-α monomer with indicated C- and N-terminus and Cys-Cys interaction [18]

As mentioned above, the active soluble homotrimer is composed of three 157-amino-acid-long monomers that are linked non-covalently. The species of amino acids, length of the chain, the liquid that surrounds the protein as well as other factors are responsible for the net-charge of the protein [19]. The so called isoelectric point (pI) defines the pH value at which a protein's net charge is neither positive nor negative. Theoretically, the isoelectric point of recombinant human TNF-α monomer is approximately 7.0 in soluble form. If the pH of the solution almost reaches the pI of the protein, precipitation can occur [20]. This can be explained by the decrease of repulsive forces due to the zero charge of the protein and simultaneously increasing of attraction forces which finally result in protein aggregation [21].

Furthermore, concentration of homotrimeric TNF-α can be measured by its absorption at 280 nm and its extinction coefficient adds up to 1.243 according to ExPASy ProtParam tool (https://web.expasy.org/cgi-bin/protparam/protparam access date: 10.04.19).

In addition, stability studies of TNF have shown that the in-vivo and in-vitro half-life of the cytokine is rather low, especially at inappropriate storage conditions [22]. In particular too high storage temperature can significantly decrease the concentration of TNF. Experiments have shown that the mean level of TNF-α in plasma stored at room temperature (24°C) for 20 days might be reduced up to 55% (Figure 3) [23].

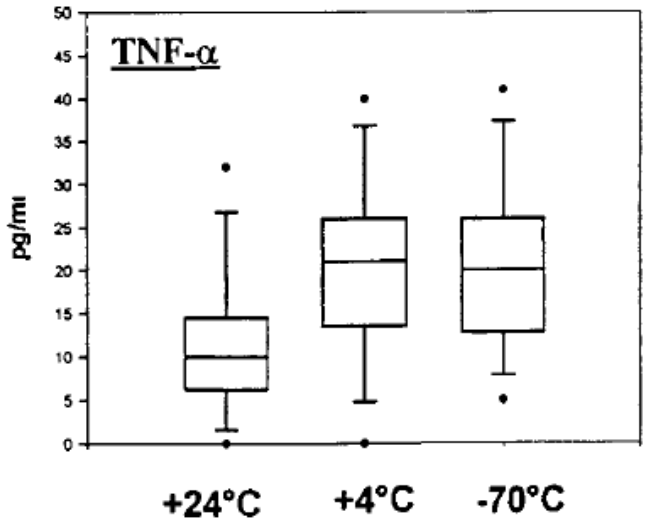

Figure 3: Titer reduction of TNF-α at different temperatures stored for 20 days [23].

In-vivo, fast degradation of TNF-α occurs within 20 minutes to half of its initial concentration. This fast clearance behavior might influences the effectiveness of the cytokine [24].

1.1.3. Clinical relevance and effects of sTNF-α

The broad variety of positive and negative physiological effects triggered by TNF-α release can be complex. Some examples of the broad variate of TNF-α effects are listed in Table 1.

Table 1: Examples of the broad range of effects of TNF-α.

Main effects of tumor necrosis factor-α	
Tumor suppressive	*Tumor promoting*
Cell survival and proliferation	Promotes cell transition
Activation of cytotoxic cells	Modulation of immune system
Maturation of dendritic cells	
Induces apoptosis	

Basically, the innate immunity system activates cytokines production and release during e.g. inflammation or infection [25]. As shown in Figure 1, sTNF-α can bind two different receptors resulting in various physiological processes. On the one hand TNFR1 is mainly responsible for the signal cascade leading to the activation of nuclear factor 'kappa-light-chain-enhancer' of activated B-cells (NF-κB cells) and cytotoxicity. On the other hand, TNFR2 mediates T-cell survival as well as proliferation. In addition, activation of other factors and cells takes place to achieve a more effective immune response [26]. However, not all effects resulting from the signal cascades are beneficial for the organisms to be protected. Defects in the lig-and-receptor signaling pathway could lead to many autoimmune disorders such as Crohn's disease, multiple sclerosis, systemic lupus and other related syndromes [26]. Furthermore, tu-mor necrosis factor plays a major role in tumor development. Due to its ability to promote cellular transformation, proliferation and angiogenesis, TNF acts as a linker between inflam-mation and carcinogenesis. In addition, concentrations of TNF found in serum as well as in tumor cells of cancer patients are nowadays used as a marker for the progress of tumor path-ogenesis and regression and is therefore essential for further prognosis [9].

Nevertheless, the ambiguous TNF effects enables various therapeutic options to cure or at least regress TNF-related diseases. By enhancing the selectivity of TNF-induced cytotoxicity the resistance of cancer cells to NF-κB mediated cell death could be circumvented. Another strategy is to fuse differently expressed antibodies (-fragments) with TNF-α to produce a fu-sion protein that features antigen binding affinity, stability as well as intact TNF-α activity [9,27]. Furthermore, the development of monoclonal antibodies (mAbs) has enabled the capture

and inactivation of TNF-α in several inflammatory diseases. A well working co-therapy is, for instance, the administration of the monoclonal antibody Adalimumab, also known under the brand name Humira, against Crohn's disease. Binding of anti-TNF mAb to its ligand inhibits the effect of TNF-α and therefore hinders the progression of the disease [28].

Summing up, intensive studies of the molecular action and signaling pathways of this cytokine could enable new possibilities to treat different human diseases [9]. Therefore, the field of protein engineering and purification also focusses on new ways to achieve better strategies for obtaining large amounts of the protein of interest in a highly pure form.

1.1.4. Purification strategies of sTNF-α

The gram-negative bacteria Escherichia coli (*E. coli*) is one of the most-used expression systems for the production of recombinant proteins. The knowledge gained in the last decades about the properties of the gram negative bacteria as well as its growth kinetics makes production nowadays straightforward [3]. By inserting an expression vector carrying the genes for TNF-α into E. coli cells relative high yields of TNF can be achieved [20].

Different strategies are described to obtain active sTNF-α in large amounts: By harvesting the cells, which produce the protein of interest intracellularly followed by disruption of the cells by sonication/homogenization all cell components are released and accessible. After second centrifugation, the supernatant consisting of the protein of interest as well as other molecules can then be separated from each other and purified by different filtration as well as chromatographic methods. Additional precipitation steps could enhance protein recovery and simplify purification [29]. This would lead to a more effective strategy to produce and purify TNF-α. A flow chart of the above described strategy is displayed in Figure 4.

Another strategy is to modify the genes expressing for TNF-α in a controlled matter. Prior to expression and production, a genetic fusion of the genes of the protein of interest with the genes expressing for e.g. a protein tag takes place. This results in an altered N-terminus that can be captured and purified with high selectivity by affinity chromatography. After this purification step an enzymatically catalyzed cleavage of the additional modifier allows the release of TNF-α. By further purification, all unwanted components can be separated from the protein of interest and thereby, a highly pure product can be achieved [30]. Economically, this process is more costly and less practical, due to the additional work necessary to fuse genes as well as cleaving and separating the tag from the protein of interest [20].

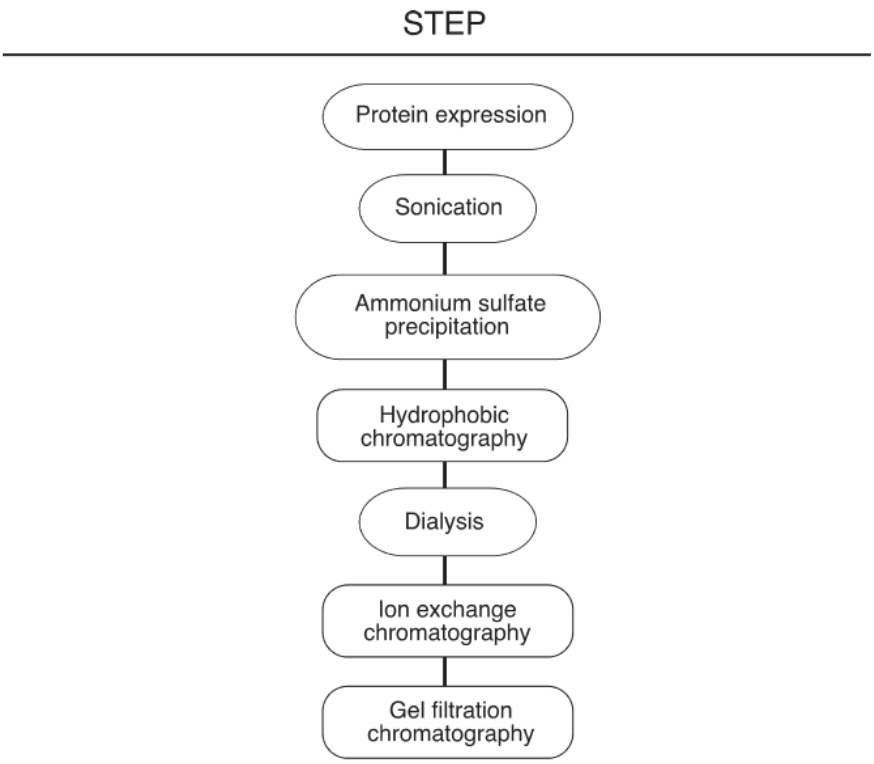

Figure 4: Flow chart of the production and purification of TNF-α [29]

Another strategy is to focus mainly on obtaining recombinant TNF-α from inclusion bodies produced by E. coli. A high expression of a protein could overburden the protein folding and quality control system of bacteria resulting in formation of aggregates. This misfolded molecules, called inclusion bodies, contain large amount of the protein of interest and can be separated easily from other host cell components [31]. As described above, after production of cells carrying the protein of interest disruption of the cells has to take place. In contrast to the prior explained strategies the pellet containing the inclusion bodies obtained after centrifugation is used for further processing. Washing with denaturing and reducing agents enables the solubilization and unfolding of proteins. Finally, refolding and purification steps allow the recovery of recombinant active TNF-α [32]. Despite the simplicity of the separation refolding TNF-α is not yet really suitable for large-scale production due to being a time-consuming procedure [20].

1.2. Principles of methods

Basically, proteins are produced intracellularly in E. coli which means that a break-up of the cells is necessary. This is most likely done by using high pressure homogenization. After successfully bursting the cells, proteins have to be separated from other intracellular as well as cell-wall components. By using centrifugation, a sufficient segregation can be achieved. Due to different properties of proteins a further separation as well as purification can be accomplished by using several chromatographic methods.

Mechanisms and principles of the used process steps all major unit operations are explained in the following section.

1.2.1. Centrifugation

Generally, one of the first steps in the separation procedure after fermentation is centrifugation. This method enables the segregation of materials that differ in density by applying a centrifugal force. Basically, this unit operation is for instance used to remove cells from the culture liquid as well as separating supernatants consisting of proteins of interest from solid components of the host. By rotating a suspension at a specific speed, particles move radially away from the axis of rotation (Figure 5). This results in a phase-separation of components that exhibit a different density [33, 34].

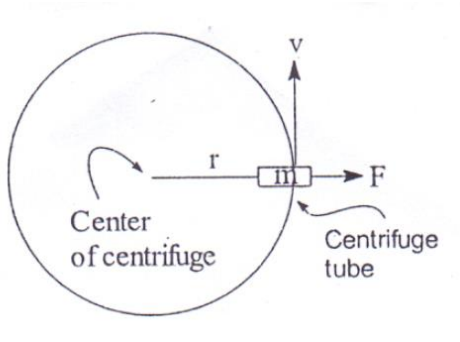

Figure 5: Principle of centrifugation: r indicates the radius of the rotation curve, v describes the direction of rotation and F indicates the centrifugal force [34].

The sedimentation velocity u_g is given by Stoke's law:

$$u_g = \frac{\rho_p - \rho_l}{18\mu} D_p^2 g \tag{3.1}$$

This equation (3.1) describes the settling velocity of a sphere in a gravitational field, where u_g is the sedimentation velocity, ρ_p and ρ_l describe the density of the particle and liquid, μ is the dynamic viscosity of the liquid, D_p is the sphere's diameter and gravitational acceleration (g). The main difference between the particle velocity in a gravitational field and in a centrifuge is the type of force acting on the particle that causes separation. Therefore, the gravitational acceleration g is replaced by the square of the angular velocity ω multiplied by the radius r of the centrifuge drum resulting in the final equation for the particle velocity u_c in a centrifuge [33].

$$u_c = \frac{\rho_p - \rho_l}{18\mu} D_p^2 \omega^2 r \tag{3.2}$$

1.2.2. High pressure homogenisation (HPH)

Due to cytoplasmic or periplasmic expression of proteins in bacteria disruption of the cells has to be performed to release the product from the cells. A unit operation that is mainly used to break up cells is high pressure homogenisation. It depends on the type of host cell as well as the type of product if this unit operation is suitable or not.

In principle, disruption is achieved by forcing cell suspensions under pressure through a slim orifice as illustrated in Figure 6. Cavitation, shear forces and pressure shock are the main factors responsible for efficient break up of cells [33,35].

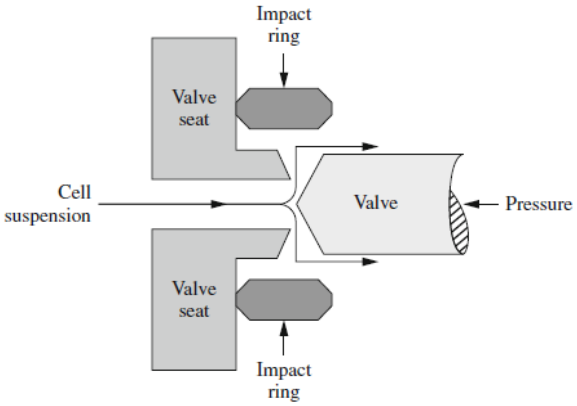

Figure 6: Principle of high pressure homogenisation [33].

To achieve better disruption, cell suspensions are frequently homogenised for more than for one passage, meaning the unit operation is performed repeatedly. Efficiency is, furthermore,

effected by pressure, temperature, number of passes, valve and impingement design as well as flow rate [36].

1.2.3. Liquid chromatography (LC)

For further identification and purification of the protein of interest with high efficiency chromatographic methods can be used. Chromatography is based on the differential adsorption of components within bead-shaped porous particles attached with different functional groups in packed beds. Basically, a mixture of components is applied onto one end of a fixed bed column and transported through the column by a so-called mobile phase. Due to different partitioning of the components between the phases separation occurs. Elution of adsorbed components is affected by feeding buffers with constant or varying modifier concentration after sample loading. A wide range of different chromatography types has been developed until today. In general, they differ in adsorption and separation principles [37,38]..

1.2.3.1. Ion exchange chromatography (IEX)

The basic principle of ion exchange chromatography is electrostatic attraction and repulsion. As described previously, the charge of a protein depends on the length and composition of its amino acid sequence as well as on the pH of the solution they are dissolved in. The isoelectric point determines the pH at which a protein's net charge is zero. If the pH of the protein solution is higher than the pI of the protein its net charge is negative, whereas a positive charge is obtained if the pH is below the pI. This phenomenon sets the basis for anion (AIEX) and cation exchange chromatography (CIEX), collectively termed IEX [38].

In general, a functional group oppositely charged as the protein of interest is immobilized on the surface of the adsorbent. This group interacts electrostatically with the charged group of the component to be separated. As the name implies, anion exchange chromatography works by replacing a negative charged group (anion) with a stronger interacting group of the same kind of charge competing for the functional group. Furthermore, ionic strength plays a major role during this exchange. By increasing the ionic strength after successfully binding the protein of interest to the ion exchange stationary phase, these components can be desorbed again. This is basically done by increasing the salt concentration in the mobile phase resulting in a competition between the salt ions and the charged groups of the proteins. The same principle works for cation exchangers dealing with positively charged groups competing for a nega-

tively charged functional group attached to the stationary phase [33,37,38]. The mechanism of binding during anion exchange chromatography is illustrated in Figure 7.

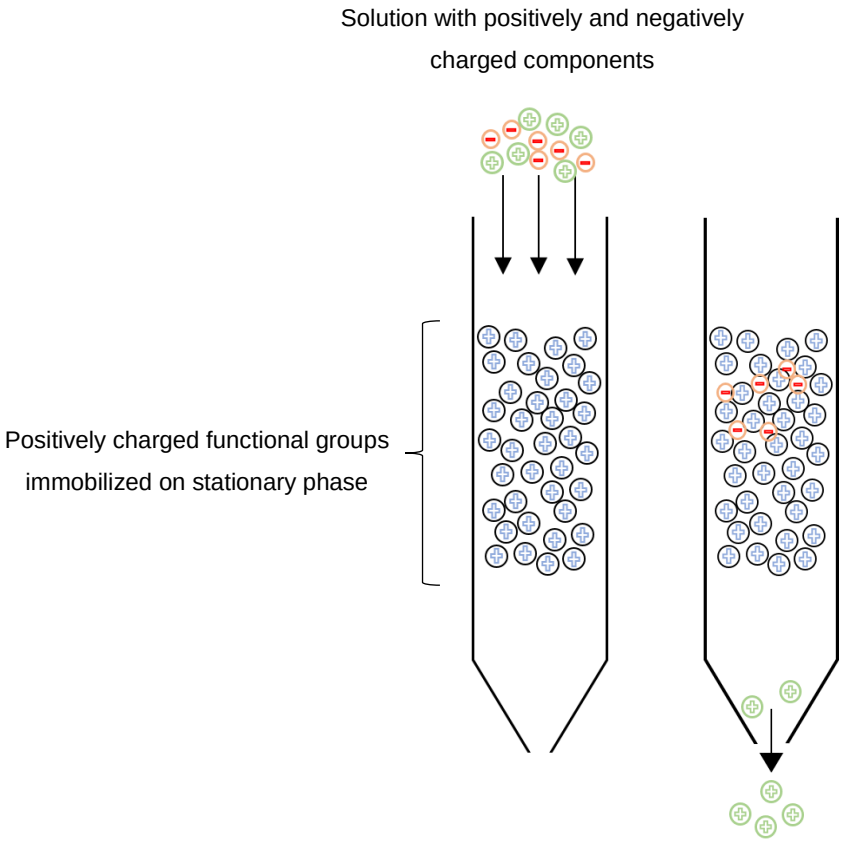

Figure 7: Principle of Anion exchange chromatography. Loading of sample and wash out of unbound proteins (own illustration).

Furthermore, based on the protonation degree of the ionogenic ligands, ion exchangers can be classified as weak or strong. Strong ion exchangers are more or less independent of pH and therefore being charged at nearly every practical pH value. However, weak ion exchangers can only be used in the pH range of 5-9 to enable effective binding [38].

1.2.3.2. Gel filtration/Size exclusion chromatography (SEC)

The principle of this unit operation is solely based on separation of components according to their molecular size and shape. Therefore, during this chromatographic method no adsorption takes place. Basically, the difference in pore space in the stationary phase enables separation components according to their molecular properties. The travelling speed of each component depends on the size of the components: large molecules are excluded from the pores and thus move faster through the column. Penetration into the pores is only possible for smaller mole-

cules and hence moving slow through the gel matrix (Figure 8) [33,37]. Longer retention time of small molecules enables for instance buffer exchange of solutions [39, 40].

Moreover, this method is mainly used as a preparative step to separate molecules, to determine their molecular weight and can therefore being used as an analytical tool as well [41].

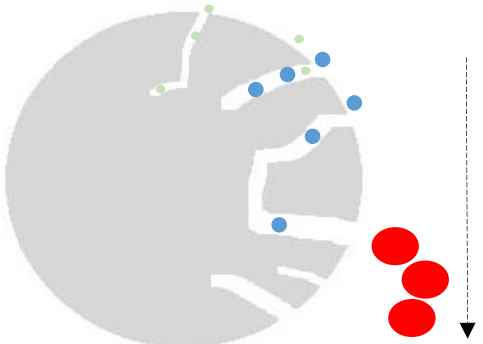

Figure 8: Principle of Size exclusion chromatography. Exclusion of larger particles of the internal pores (own illustration)

1.2.4. High performance liquid chromatography (HPLC)

One of the main differences of HPLC to normal liquid chromatography is the diameter of the particles of the stationary phase. By using smaller particles, dispersive effects are greatly reduced resulting in enhanced column performance. A major disadvantage of HPLC compared to LC is the increase of back pressure caused by the smaller particle size and decreased space between these particles. Therefore, it is mainly used as a sensitive analytical technique but preparative use with particles in the intermediate size range is also common. Moreover, the separation principles behind HPLC methods do not differ from the various LC techniques [42,43].

1.2.5. Sodium dodecyl sulfate polyacrylamide gel electrophoresis (SDS-PAGE)

By using electrophoretic methods complex mixtures containing proteins can be segregated. An electric current enables the movement of charged molecules through a polyacrylamide gel matrix. Sodium dodecyl sulfate is a negatively charged detergent that causes denaturation of non-disulfide linked structures resulting in solubilized proteins exhibiting a negative charge as well. Furthermore, the electric field causes migration of the charged molecules towards a

positive pole, called anode. The complex polyacrylamide gel matrix hinders the migration of larger molecules resulting in a shorter covered distance. Therefore, separation of differently sized components takes place. Staining of proteins is performed with specific dyes. This allows an estimation of the molecular weight of unknown molecules as well as identification of the proteins of interest [44].

1.2.6. Protein immunoblotting methods

For the determination whether a specific antigen is present or not immunoblotting methods can be helpful. This is done by blotting macromolecules that have been separated electrophoretically onto a membrane (western blot) or by directly applying the solution of interest on the membrane as a dot (dot blot). The membrane is then incubated with a first antibody specific for the antigen of interest. A second antibody-enzyme conjugate with high affinity to the first antibody is then applied to bind the antigen-antibody complex immobilized on the membrane. After adding a chromogenic substrate, which can be converted by the present enzyme, detection of the bound antigen is possible by a color reaction. Furthermore, several washing steps of the membrane during the procedure are necessary to block unspecific binding. This detection method can be used in different areas of immunology and other related fields [45].

1.3. Aim

The aim of the present study was to establish an effective purification strategy for TNF-α from *E. coli*. The starting point was a published procedure based on a combination of anion- and cation exchange chromatography. The initial goal was to reproduce this procedure, further characterize adsorption kinetics and extend the study to other, potentially better performing, ion exchange resins. However, during the work an unexpected problem occurred: a heterogeneous aggregate also containing parts of TNF-α was present in the feed material that significantly interfered with TNF-α binding and dropped purification efficiency. As such, a significant part of this work was then spent on deeper investigation of the nature of this aggregate. Nevertheless, the main task of TNF-α purification by using the two ion exchange chromatography methods could be fulfilled.

2. Material and Methods

2.1. General procedures

2.1.1. Host strain

Fed-batch fermentation of TNF-α was done in another working group of the Department of Biotechnology. As host strain Escherichia coli (BL21) was used, which basically expresses the protein of interest periplasmically. Furthermore, *E. coli* carried the plasmid pET30a(cer)_ompA_TNFa-sol17, which means that active TNF-α containing an outer membrane A leader is produced. The ompA is responsible for the transport to the periplasmic space. This leader should be detached after successfully transporting the protein to its terminal.

2.1.2. Harvest and high-pressure homogenization

2.1.2.1. Materials and instrumentation

- Centrifuge - Avanti JXN-26 Centrifuge with a fixed angle rotor (JLA-10.500 max 10000 rpm) and centrifuge buckets (BECKMAN COULTER; Brea, USA)
- Lab balance- ENTRIS5201-1S (Sartorius; Göttingen, Germany)
- -20 °C Freezer
- Buffer for re-suspending/homogenization step: 20 mM Tris, 1mM Titriplex® III (both Merck; Darmstadt, Germany) dissolved in HQ water and adjusted to pH 8.0 – 9.5 with HCl
- Ice for cooling
- Magnetic mixer – MR Hei – Standard Mixer (Heidolph; Schwabach, Germany)
- Overhead mixer – VOS-14 (VWR; Radnor, USA)
- Two stage homogenizer Panda Plus (GEA Niro Soavi; Düsseldorf, Germany)
- Flow-cooler: 1175PD Recirculator (VWR; Radnor, USA)
- Flushing solution: tap water
- Sanitization solution: 0.1M NaOH (Merck; Darmstadt, Germany) dissolved in tap water
- Storage solution: 20% EtOH diluted in tap water

2.1.2.2. Method

By using the balance, the fermentation broth was portioned to 200 mL volumes directly in the centrifuge buckets. A difference of 0.1 g of each filled bucket was tolerated due to the sensitivity of the centrifuge. The pre-cooled centrifuge (to 4°C) was then loaded and prior to starting parameters were set to 10000 rpm and duration was adjusted to 20 minutes. The pellet was then transferred into freezer bags and stored in the -20°C freezer.

For re-suspension and homogenization, the balance was used to weigh in frozen cells and buffer was added up to obtain in a suspension containing 25 g/L dry cell weight. Constant cooling was achieved by transferring the flask into a bigger beaker, which was filled up with ice. By stirring the suspension for ~4 hours with the magnetic or overhead mixer a homogenous solution was achieved. In the meantime, the homogenizer was flushed with tap water to remove the storage solution. This step was done without applying any kind of additional pressure. To determine the flow rate of the homogenizer, a flow rate test with water was done by adjusting the first stage to 70 bar and the second stage to 700 bar. The test should result in a flow rate of approximately 200 ml/min at an adjusted frequency of 50 Hz. After flushing the system with the re-suspension/homogenization buffer the suspension was applied and the stages were again adjusted to 70/700 bar. Homogenization of the solution was performed for 2 passages, afterwards pressure was released. If cooling of the device was required a recirculating chiller had been used, which was set to 4°C. The homogenate was centrifuged in a pre-cooled (4°C) centrifuge for 30 minutes at 10000 rpm and finally the supernatant was stored in the freezer at -20°C. Cleaning of the homogenizer was done by flushing the apparatus primary with water for several times. Sanitization was performed by flushing the system with 0.1 M NaOH. Finally, the apparatus was stored in 20% EtOH.

2.2. Purification of TNF-α

2.2.1. Äkta explorer 100 system

For all liquid chromatography steps the Äkta explorer 100 system (GE Healthcare; Chicago, USA) was used. The basic features and flow diagram are illustrated in Figure 9.

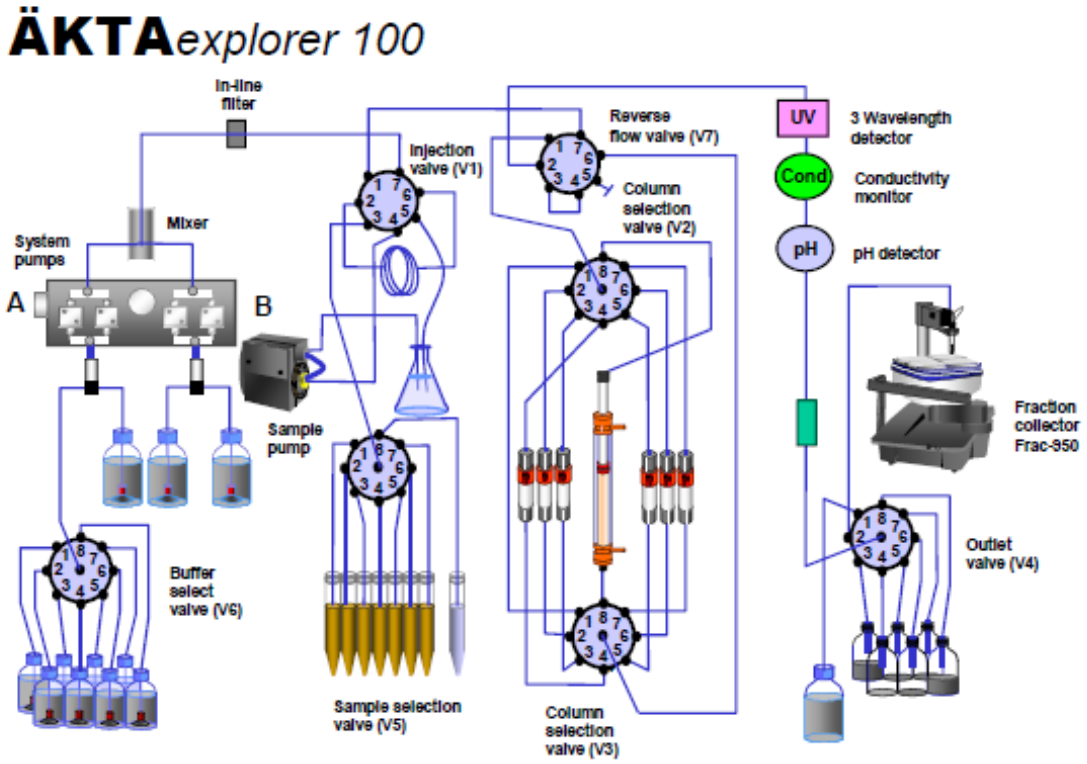

Figure 9: Valve Diagram of Äkta explorer 100 (Source: Aekta Valve Diagrams)

Basically, the system consisits of two pumps, that can be operated separately. As the name implies, this Äkta system is configured to be used up to flow rates of 100 mL/min and 100 bar. Furthermore, absorbance, conducitivity and pH is measured on-line.

The software controlling the system was Unicorn 3.0.

2.2.2. Salt exchange via gel filtration

2.2.2.1. Materials and instrumentation

- Microcentrifuge: Centrifuge 5415R (Eppendorf; Hamburg, Germany)
- Millex GV Filter 0.22 µm 33 mm (Merck; Darmstadt, Germany)
- Äkta Explorer 100 with Frac 950 (GE Healthcare; Chicago, USA)
- Sephadex G25, packed in XK 16/20 coulmn, 1 CV = 100.31 mL
- Sephadex G25, pre-packed in PD10 column (GE Healthcare; Chicago, USA)
- Buffer: 20 mM Tris (Merck; Darmstadt, Germany) dissolved in HQ water and adjusted to pH 8.5 with HCl and 20 mM MES (Sigma; St. Louis, USA) dissolved in HQ water and adjusted to pH 6.0 with NaOH
- Sanitization solution: 0.1 M NaOH (Merck; Darmstadt, Germany) dissolved in HQ water
- Storage solution: 20% EtOH diluted in HQ water

2.2.2.2. Method

Prior to salt exchange, the frozen supernatant was thawed and further transferred to 2 mL reaction tubes. Rotation of the pre-cooled (4°C) microcentrifuge were adjusted to 13.200 rpm and duration was set to 20 minutes.

For larger volumes, the Sephadex G25 column was equilibrated with the respective buffer until conductivity stayed constant. The flow rate was kept constant at 1 mL/min during the whole salt exchange step. After successfully separating residual cell debris from the supernatant, the solution was loaded via a filter into a suitable super loop, which had been flushed and connected to the Äkta system. A sample volume corresponding to one third of the column volume was applied to the Sephadex G25 column per run during salt exchange step. Sample exchanged into the new buffer was then collected by using the fraction collector. The column was flushed until absorbance returned to zero. For storage the Sephadex column with 20% EtOH.

For smaller volumes, equilibration of the PD10 columns was achieved by applying approximately 15 mL of the buffer onto the column. Salt exchange was further performed by applying 2.5 mL of the sample containing the old buffer onto the column and eluting the larger proteins out with 3.5 mL of the new buffer. After flushing the column with water for several CVs the desalting column was used again for another salt exchange step or sanitized by ap-

plying 0.1 M NaOH. Storage condition were afterwards achieved by washing the column with 20% EtOH.

2.2.3. Anion exchange chromatography

2.2.3.1. Materials and instrumentation

- Äkta Explorer 100 with Frac 950 (GE Healthcare; Chicago, USA)
- Capto Q Impress resin packed in Tricorn 5/55 or Source 15Q resin packed in Tricorn 5/100 (both GE Healthcare; Chicago, USA) or
  Praesto Q35 jetted resin (Purolite; Bala Cynwyd, USA) packed in Tricorn 5/100
- Millex GV Filter 0.22 µm 33 mm (Merck; Darmstadt, Germany)
- Equillibration buffer A: 20 mM Tris (Merck; Darmstadt, Germany) dissolved in HQ water and adjusted to pH 8.5 with HCl
- Elution buffer B: 20 mM Tris 1 M NaCl (Merck; Darmstadt, Germany) dissolved in HQ water and adjusted to pH 8.5 with HCl
- Regeneration buffer C: 0.1 M NaOH (Merck; Darmstadt, Germany) dissolved in HQ water

2.2.3.2. Method

Prior to the AIEX step, the homogenate was clarified by using centrifugation and afterwards desalted on a Sephadex G25 as described in the sections above. All steps were performed at a flow rate of 1 mL/min. After the system was flushed with buffer A the anion exchange column was equilibrated with 4 CV of the equilibration buffer. 15 mL of samples were loaded onto the column and after loading, buffer A was used to wash unbound components off the column. This washing step was performed for 10 CVs. Elution of the bound proteins was obtained by washing the column with 30% of buffer B for 10 CVs. Buffer B was afterwards raised to a concentration of 100% linearly in 4 CV. The high salt concentration was then kept for 5 CVs. Regeneration was performed by washing the system with buffer C followed by flushing the column for 4 CVs. To recondition the column, 100% of buffer B was applied for 2 CVs followed by an equilibration step with buffer A for 4 CVs.

The procedure is summarized in Table 2:

Table 2: Steps performed during Anion exchange chromatography - step gradient

Step	Buffer type and %	Duration (in CV)
Column equilibration	A: 100	4
Sample load	A: 100	15 mL loaded
Unbound wash	A: 100	10
Step elution	A: 70 B: 30	10
High salt elution	B: 30-100	4
High salt wash	B: 100	5
Regeneration	C: 100	4
Recondition with salt	B: 100	2
Re-equilibration	A: 100	4

2.2.4. Cation exchange chromatography

2.2.4.1. Materials and instrumentation

- Äkta Explorer 100 with Frac 950 (GE Healthcare; Chicago, USA)
- Mono S prepacked in Tricorn 5/50 (GE Healthcare) – 1 CV = 0.982 mL
- Millex GV Filter 0.22 µm 33 mm (Merck; Darmstadt, Germany)
- Equillibration buffer A: 20 mM MES (Sigma; St. Louis, USA) dissolved in HQ water and adjusted to pH 6.0 with NaOH
- Elution buffer B: 20 mM MES (Sigma; St. Louis, USA) 1 M NaCl (Merck; Darmstadt, Germany) dissolved in HQ water and adjusted to pH 6.0 with NaOH
- Regeneration buffer C: 0.1 M NaOH (Merck; Darmstadt, Germany) dissolved in HQ water

2.2.4.2. Method

Prior to the cation exchange run, the eluate of the anion exchange chromatography run was desalted by using the Sephadex G25 in PD10 desalting columns as described above. Thereby, the proteins were transferred into 20 mM MES pH 6.0 that enables binding on the cation exchange resin. All further procedures were performed analogously to the AIEX step gradient illustrated in Table 2. In addition, as flow rate 1 mL/min was chosen for all steps during CIEX step gradient elution. Elution was performed with linear gradient from 0 to 0.4 M NaCl over 14 CV, followed by a linear gradient from 0.4 to 1.0 M NaCl over 4 CV. Analytics were performed as described in the following section.

2.3. Analytics

2.3.1. Size exclusion chromatography

2.3.1.1. Materials and instrumentation

- Alliance® HPLC - e2695 with 2489 UV/VIS Detector (Waters; Milford, USA)
- HPLC vials (Sigma; St. Louis, USA)
- Superdex 75 10/300 GL (GE Healthcare; Chicago, USA) - 1 CV = 23.562 mL
- Millex GV Filter 0.22 µm 13 mm (Merck; Darmstadt, Germany)
- Buffer: 1x PBS pH 7.4 (Merck; Darmstadt, Germany)
  (0.137 M NaCl, 0.0027 M KCl, 0.01 M Na_2HPO_4, 0.0018 M KH_2PO_4)
  Chemicals dissolved in HQ water

2.3.1.2. Method

Equilibration of the SEC column was performed for 1.5 CV. The flow rate was set to 0.5 mL/min. 10-100 µL of the filtered sample were loaded onto the column. Elution with the main buffer was performed until all components were washed out of the system signalized by a flattened conductivity and absorbance curve.

2.3.2. Sodium dodecyl sulfate polyacrylamide gel electrophoresis

2.3.2.1. Materials and instrumentation

- Invitrogen XCell Sure Lock™ (Thermofischer; Waltham, USA)
- Invitrogen Novex Mini-Cell (Thermofischer; Waltham, USA)
- Electrophoresis Power Supply EPS301 (GE Healthcare; Chicago, USA)
- 0.5 mL reaction tubes (Eppendorf; Hamburg, Germany)
- Minispin centrifuge (Eppendorf; Hamburg, Germany)
- Thermomixer comfort with 0.5 mL block (Eppendorf; Hamburg, Germany)
- Invitrogen NuPAGE 4-12% Bis Tris Gel (Thermofischer; Waltham, USA)
- Dilution buffer: 20 mM Tris pH 8.5 or 1x PBS pH 7.4
- NuPAGE reducing agent DTT.
- RO-H_2O
- NuPAGE LDS sample buffer

- Fixing solution: 500 mL 96% ethanol, 100 mL glacial acetic acid filled up to 1000 mL with RO-H_2O
- Staining solution: 250 mL 96% ethanol, 80 mL glacial acetic acid, 1.16 g Coomassie Blue R250 filled up to 1000 mL with RO-H_2O
- Destaining solution: 250 mL 96% ethanol, 80 mL glacial acetic acid filled up to 1000 mL with RO-H_2O
- Running buffer: 1x MES SDS running buffer
- Mark12 standard (Thermofischer; Waltham, USA)

2.3.1.2. Method

13 µL of each sample were pipetted into a 0.5 mL Eppendorf tube. If dilution was required, the sample was mixed with the original buffer of the sample. Next, 5 µL of the LDS sample buffer and 2 µL of the reducing agent or RO-H_2O, if additional reduction was not necessary, were added. The tubes were shortly spun down with the centrifuge and afterwards incubated for 10 minutes in the thermomixer at 70°C with shaking of 600 rpm. A short spin-down allowed accumulation of the partly evaporated liquid drops. The NuPAGE Gel was rinsed with water and placed into the Mini-cell chamber. After the chamber was filled with running buffer, the samples were loaded into the wells of the gel. For easier characterization of the separated components a Mark12 standard was as well loaded onto the gel. Parameters of the electrophoretic power suppliers were set to 200 V and 400 mA and duration was adjusted to 50 minutes. After successful separation the gel was uncased and incubated with fixing solution for 30 minutes on a shaker. The liquid was afterwards replaced by staining solution and staining was performed for 30 minutes on the shaker. Next, the Coomassie blue was discarded and de-staining solution added. This de-staining step was performed twice for 1 hour on the shaker. After background of the gel was de-coloured properly, a scanner was used for the purpose of recording and evaluation.

2.3.3. Dot blot

2.3.3.1. Materials and instrumentation

- TBS: 20 mM Tris, 150 mM NaCl (Merck; Darmstadt, Germany) adjusted to a pH of 7.4 by addition of HCl
- TBS-T: 0.05% Tween20 (Sigma; St. Louis, USA) diluted in TBS
- BSA/TBS-T: 0.1% BSA (Sigma; St. Louis, USA) was dissolved in TBS-T
- Blocking solution: 5% BSA (Sigma; St. Louis, USA) dissolved in TBS-T
- Nitrocellulose membrane (BIO-RAD; Hercules, USA)
- Adalimumab (Department of biotechnology, BOKU) diluted in BSA/TBS-T to a concentration of 5 µg/mL
- Anti-Human IgG (whole molecule) − alkaline phosphatase antibody produced in goat (Sigma; St. Louis, USA) 1:1000 dilution in BSA/TBS-T
- Substrate BCIP®/NBT (Sigma; St. Louis, USA) dissolved in 50 mL RO-H_2O
- Stop reagent: RO-H_2O

2.3.3.1. Method

The nitrocellulose membrane was divided into segments by drawing a grid. 2 µL of each sample was transferred onto marked segments and the membrane was dried for approximately 30 minutes. Afterwards, the membrane was incubated in blocking solution for 30 minutes on the shaker at RT to inhibit un-specific binding. Next, the diluted Adalimumab solution was applied onto the membrane and again incubated for 30 minutes on the shaker. Unbound antibody was washed away by incubating the membrane with TBS-T for 5 minutes on the shaker repeated for three times. Incubation of the membrane with the anti-human IgG was performed for 30 minutes at RT on the shakers. By washing three times with TBS-T (15 min once and 5 min twice) followed by one wash with TBS for 5 minutes on the shaker unbound antibodies had been removed. Finally, the membrane was incubated with the substrate solution and the reaction was stopped after dots got stained dark blue (after 1-2 minutes) by adding RO-H_2O.

2.3.4. TNF- α quantification and purity determination

2.3.4.1. Materials and instrumentation

- Recombinant human TNF-α standard (Peprotech; Rocky Hill, USA)
- Alliance® HPLC - e2695 with 2489 UV/VIS Detector (Waters; Milford, USA)
- HPLC vials (Sigma; St. Louis, USA)
- Stabilization: 1.8 mg Lactalbumin (Sigma; St. Louis, USA)
- Superdex 75 10/300 GL (GE Healthcare; Chicago, USA) – 1 CV = 23.562 mL
  or TSK-GEL SAX (TOSOH Bioscience; Tokyo, Japan) – 1 CV = 4.241 mL
- Running buffer for Superdex 75: 1x PBS pH 7.4 (Sigma; St. Louis, USA)
  (0.137 M NaCl, 0.0027 M KCl, 0.01 M Na_2HPO_4, 0.0018 M KH_2PO_4)
- SAX Equillibration buffer A: 20 mM Tris (Merck; Darmstadt, Germany) dissolved in HQ water and adjusted to pH 8.5 with HCl
- SAX: Elution buffer B: 20 mM Tris 1 M NaCl (Merck; Darmstadt, Germany) dissolved in HQ water and adjusted to pH 8.5 with HCl

2.3.4.2. Method

The purchased TNF-α standard was diluted and reconstituted according to the provided certificate of analysis. Furthermore, the diluted standard was partitioned into 6 vials containing the same amount of the protein of interest in each tube. The solution of one tube was filtered and transferred into the HPLC vial. After equilibration of the column was achieved the following runs were performed: 10, 20, 50 and 100 µL sample load. Flow rate for the Superdex 75 column was set to 0.5 mL/min

For the TSK-gel SAX column, the method was performed analogously to the AIEX purification step. Elution was achieved by applying a linear gradient (0-0.5 M) for 38 minutes followed by a linear salt increase up to 1.0 M NaCl. Flow rate was set to 1 mL/min. The same sample volumes as for the Superdex 75 SEC column were applied.

In addition, by integrating the obtained absorbance peaks, the area was determined and therefore a calibration curve was set up, which was further used to quantify TNF-α in the samples.

2.4. Characterization of aggregates

2.4.1. Aggregate binding behavior - Anion exchange chromatography

2.4.1.1. Materials and instrumentation

Same materials as described in the section above were used.

2.4.1.2. Method

Three runs were performed with different sample volumes loaded: 10 mL, 20 mL and 38 mL. The wash unbound step was done manually. Elution was performed analogously as described in the anion exchange chromatography section. The eluates were analyzed via SEC-HPLC method on Superdex 75 as well as on SDS-PAGE.

2.4.2. Stability of aggregates

2.4.2.1. Materials and instrumentation

- 8 M Urea (Sigma; St. Louis, USA))
- Rotator: SB3 (Stuart; Staffordshire, USA)
- Vortex: Genius 3 (IKA; Staufen, Germany)
- Microcentrifuge: Centrifuge 5415R (Eppendorf; Hamburg, Germany)
- Thermomixer comfort with 1.5 mL block (Eppendorf; Hamburg, Germany
- Alliance® HPLC - e2695 with 2489 UV/VIS Detector (Waters; Milford, USA)
- Superdex 75 10/300 GL (GE Healthcare, Chicago, USA) – 1 CV = 23.562 mL
- Millex GV Filter 0.22 µm 13 mm (Merck; Darmstadt, Germany)
- Main buffer: 1x PBS pH 7.4 (Merck; Darmstadt, Germany)
  (0.137 M NaCl, 0.0027 M KCl, 0.01 M Na_2HPO_4, 0.0018 M KH_2PO_4)
  Chemicals dissolved in HQ water

2.4.2.2. Method

A series of different urea concentrations were mixed with the anion exchange chromatography flow through containing the aggregate according to the Table 3.

Table 3: Urea stability series - pipetting schema

Volume of 8M Urea (mL)	Volume of dH_2O added (mL)	Sample volume (mL)	Final urea concentration (mol/L)
0.625	0.375	1.0	2.5
0.5	0.5	1.0	2.0
0.375	0.625	1.0	1.5
0.25	0.75	1.0	1.0
0.125	0.875	1.0	0.5
0	1.0	1.0	0

The solutions were constantly mixed for 20 hours on the rotator at 4°C (cold storage room). After a short spin-down of each reaction tube the supernatant was filtered and filled into HPLC vials. Prior to sample load, the SEC column was equilibrated with 1x PBS. Next, 10 µL of each solution were further analyzed on the Superdex 75 column. The flow rate was 0.5 mL/min.

Furthermore, the stability of the AIEX eluate containing the homotrimeric TNF-α was tested for the optimal urea concentration by diluting the sample with 0.5 mL of the Urea stock solution and 0.5 mL RO-H_2O. All further procedures were performed analogously to the aggregate urea stability approach described above.

For investigating the heat stability of the aggregates, 1.5 mL of the homogenate was tested by varying time and temperature summarized in Table 4.

Table 4: Schema of set conditions during heat precipitation

Temperature (°C)	Time (min)
60.0	5
	10
	15
70.0	5
	10
	15
80.0	5
	10
	15

Furthermore, the reaction tubes were put into the thermomixer for a specific time at a pre-set temperature. After cooling down, the suspensions were centrifuged for 15 minutes at 13.200 rpm. In a next step the supernatants were measured via HPLC analogously as described for the urea stability test. Moreover, an untreated homogenate was measured as well for obtaining a reference.

3. Results and Discussion

3.1. Analytics of a purchased TNF-α standard

For the determination of the analytical characteristics of trimeric TNF-α a purchased standard was used. This standard was analyzed by an analytical SEC-HPLC method on Superdex 75 (Figure 10), an analytical AIEX-HPLC method on the TSK-gel (Figure 11), and by separation and visualization on SDS-PAGE (Figure 12).

Prior the analysis, the purchased standard was diluted and reconstituted according to the provided manual. 0.1% α-lactalbumin was added for a better stability of the protein of interest.

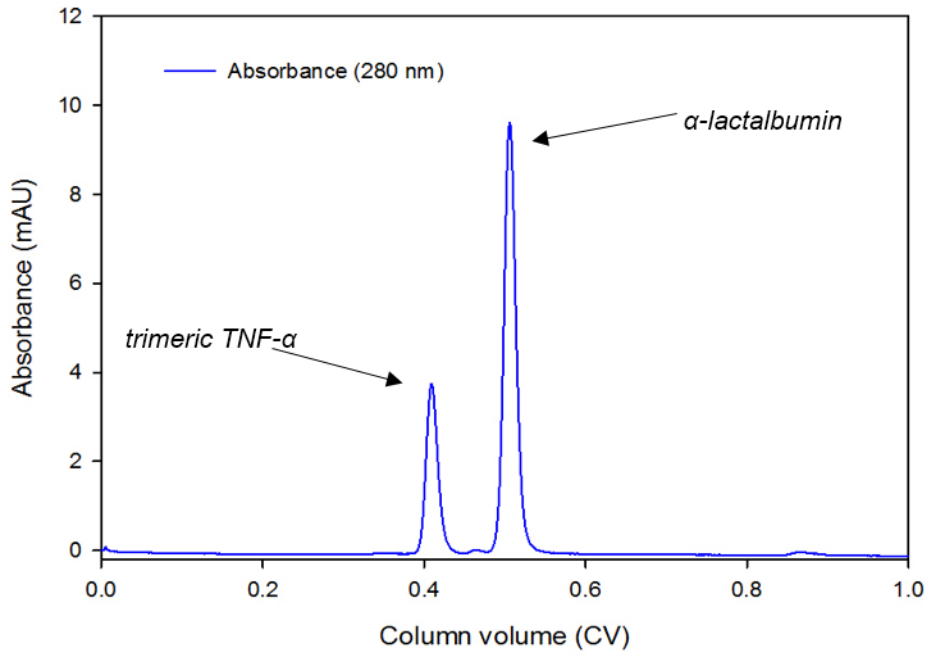

Figure 10: Analytical SEC-HPLC of TNF-α standard on Superdex 75. Load: 10 µL; 1 CV = 23.562 mL; Retention time of ~0.41 CV of trimeric TNF-α. α -Lactalbumin retention time of 0.5 CV.

The analytical SEC-HPLC on Superdex 75 showed a retention time of approximately 0.41 CV for the trimer TNF-α, approximate molecular weight of 51 kDa. (Figure 10). The second peak at 0.5 CV corresponds to α –lactalbumin, with a molecular weight of 14.2 kDa.

The elution behavior of the trimeric TNF-α standard was also determined by the analytical AIEX-HPLC method on the TSK-gel SAX column. 10 µL of the commercial standard were loaded onto the column. Trimeric TNF-α was eluted at a buffer B concentration of 0.11-0.12 M NaCl The more acidic α-lactalbumin was eluted at an elution buffer concentration of approximately 0.85 M NaCl (Figure 11).

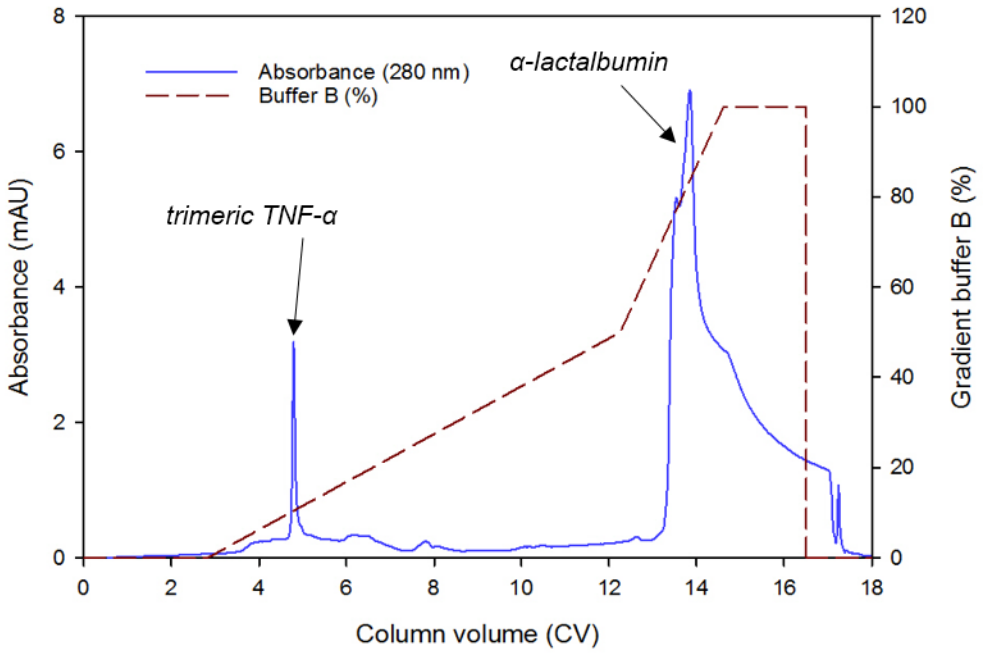

Figure 11: Analytical AIEX-HPLC of TNF-α standard on TSK-gel. Load: 10 µL; 1 CV = 4.241 mL; elution of TNF-α at 0.11-0.12 M NaCl.

The background noise of the absorbance during elution was possibly caused by the increase of salt. TNF-α standard was also analyzed by SDS-PAGE to investigate if the trimeric TNF-α would get reduced to its monomers under denaturing conditions. Three dilutions of the commercial standard were heated in presence of SDS and separated by SDS-PAGE (Figure 12).

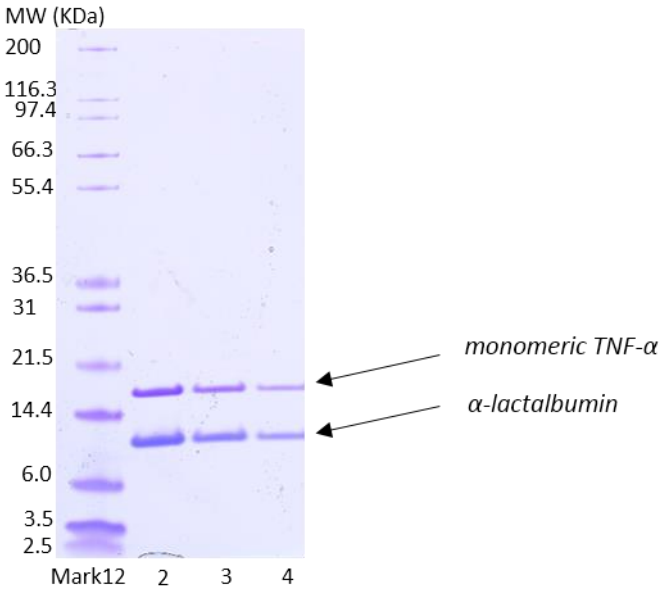

Figure 12: SDS-PAGE of trimeric TNF-α standard under denaturing conditions. Lane 1: Mark12 ladder; lane 2: undiluted standard; lane 3: 1:2 diluted standard; lane 4: 1:4 diluted standard; dilution was performed by adding 20 mM Tris pH 8.5.

In all three dilutions of the commercial TNF-α standard (Figure 12, lane 1 to 3, in the order of decreasing protein concentration) two bands were visualized. One at an approximate mass of 17 kDa, which would correspond to the mass of the monomeric TNF-α, and the second one at approximately 11 kDa which corresponds to the added α-lactalbumin. No band of the trimeric TNF-α (~51 kDa) could be visualized after denaturation. Therefore, it can be concluded that the trimeric TNF-α was fully reduced to its monomeric units.

All obtained results were used for further identification of trimeric TNF-α in the received E. coli fermentation.

3.1.1 Quantification of the standard via Superdex 75/ TSK-gel SAX

For process characterisation the quantification of TNF-α was carried out by the established SEC-HPLC method on the Superdex 75 column and AIEX-HPLC method on the TSK-gel SAX. For that purpose, calibration curves were set up relating the peak area to the amount of applied TNF-α standard. The standard curve as well as the linear equation are displayed in Figure 13.

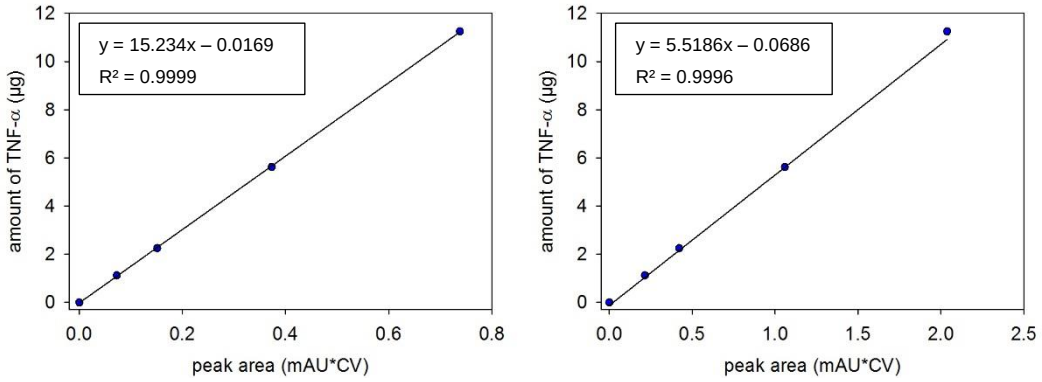

Figure 13: Calibration curves for TNF-α standard quantification by analytical SEC-HPLC on Superdex 75 (left figure) and by analytical AIEX-HPLC on TSK-gel SAX (right figure). 10-100 µL load.

For all subsequent TNF-α quantifications the linear equation y = 15.234x – 0.0169 was used for the analytical SEC-HPLC method, while the linear equation y = 5.5186 x – 0.0686 was used for the analytical AIEX-HPLC.

Due to the linear relationship between absorbance and concentration to a certain degree, which was defined by the Beer-Lambert law, concentrations beyond the values of the calibration curves were as well calculated with the equations.

3.2. Development of the strategy for preparative purification of TNF-α

First trials of purification were performed according to Zhang et al. [20], who described a strategy involving homogenization, AIEX, followed by CIEX. They used SEC-HPLC and SDS-PAGE analytics to identify and characterize TNF-α.

The buffer systems were prepared analogously to the procedure mentioned above. After cell disintegration by high pressure homogenization and subsequent clarification by centrifugation the *E.coli* homogenate was loaded onto the DEAE AIEX column (Figure 14).

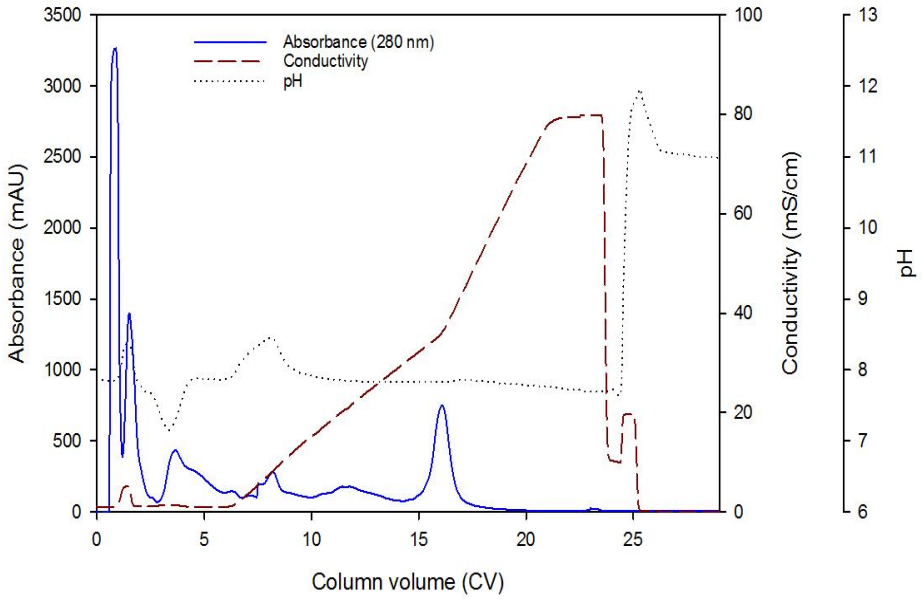

Figure 14: Homogenate directly loaded onto DEAE Sepharose FF. Load: 2 mL; 1 CV = 2.041 mL; Dotted line indicates the pH curve – during loading step pH too close to isoelectric point of TNF-α. Flow through collected from 0-6 CV; Eluate collected from 6-13 CV.

The flow through and eluate fractions were further analyzed by analytical SEC-HPLC on Superdex 75 (Figure 15).

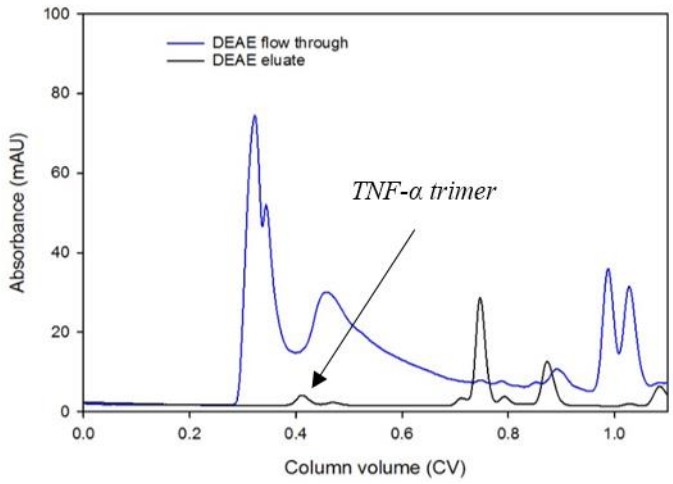

Figure 15: Analytical SEC-HPLC on Superdex 75 of flow through and eluate of DEAE run as shown in Figure 14 - 100 µL load. 1 CV = 23.562 mL.

In contrast to the results published by Zhang et al., the dominant amount of TNF-a trimer was found in the flow through fraction (Figure 15, solid blue line) and only a minor fraction of the target protein was bound to the resin and therefore found in the eluate (Figure 15, solid black line).

The manual determination of the pH in the loading solution showed a pH of 7.22, which was too close to the isoelectric point of the protein. This might have been a reason for the low binding of the trimeric TNF-α obtained for the separation on the DEAE Sepharose FF (Figure 14). After one day of storage at 4°C the pH of the homogenate even dropped to a pH value of 6.88. This acidification of the homogenate was potentially caused by host cell components of *E. coli* and further reduced the product binding to the resin.

The pH drop in the homogenate due to storage was compensated by the implementation of a pH adjusting step prior the loading to enable efficient binding. As a first approach, the homogenates were diluted to a final pH value of 8.0 and 8.5 with 20 mM Tris. This led to a 1:3 dilution of the original solution. In a next step, these solutions were loaded onto the DEAE column. The overlay of the corresponding chromatograms is shown in Figure 16.

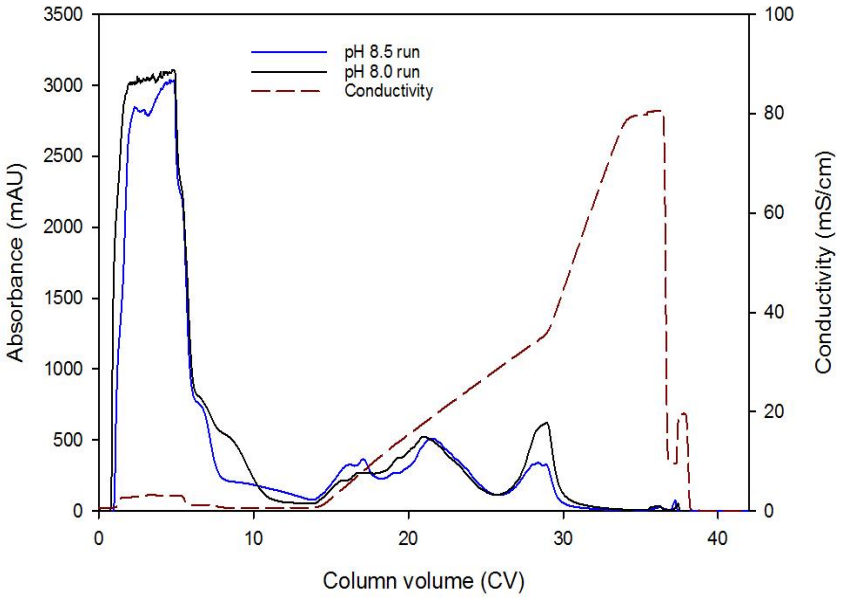

Figure 16: Comparison of separation of homogenates adjusted by dilution to pH 8.0 (solid black line) or pH 8.5 (solid blue line) prior loading to DEAE Sepharose FF. Load: 5 mL; 1 CV = 2.041 mL; Influence of pH on binding behavior - better binding achieved at pH 8.5.

Both methods did not lead to sufficient binding of TNF-α trimer to the DEAE Sepharose which was confirmed by SEC-HPLC and SDS-PAGE analytics (data not shown).

As a second approach the strong AIEX resin, Source 15Q, was tested in comparison to the weak AIEX resin DEAE Sepharose FF. Homogenates adjusted to a pH of 8.5 and untreated homogenates were loaded and eluted by a linear salt gradient. The overlay of the corresponding chromatograms is shown in Figure 17.

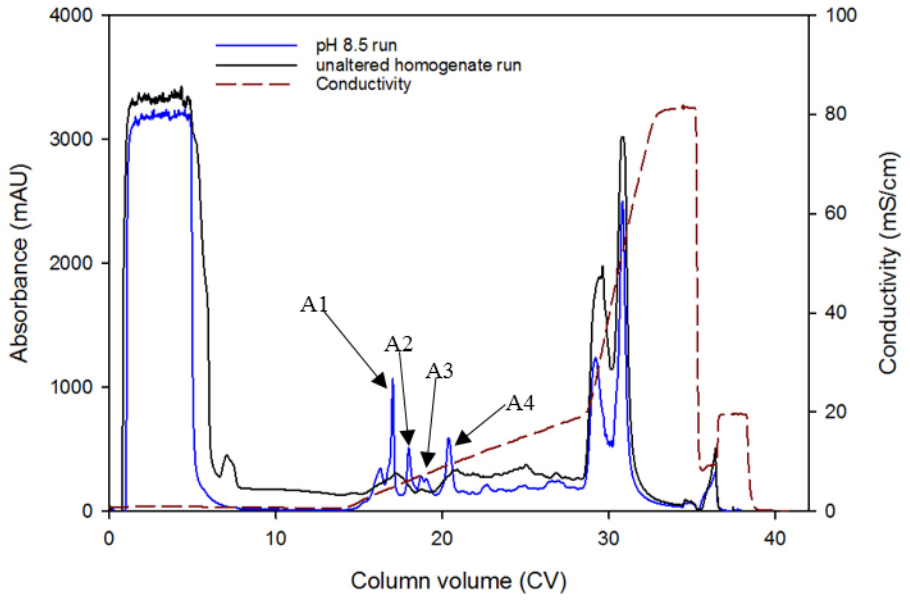

Figure 17: Separation of untreated homogenate (black solid line) and homogenate adjusted by dilution to pH 8.5 (blue solid line) prior loading to Source 15Q. Load: 9 mL; 1 CV = 2.041 mL;

The fractions A1-A4 indicated in Figure 17 were analyzed by SDS-PAGE (Figure 18). TNF-α monomer (17 kDa band) was found in fractions A2-A4 (Figure 18, lane 4 to 6). A possible explanation for this behavior could be the formation of heteromers consisting of TNF-α and other proteins resulting in elution at different salt concentrations. During analysis by SDS-PAGE this heteromers were separated by the denaturing conditions into the individual components.

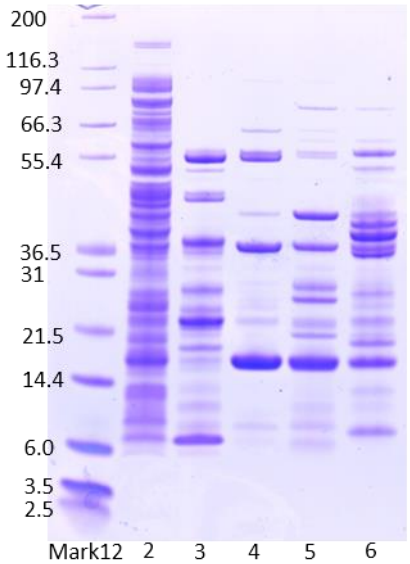

Figure 18: SDS-PAGE of the Source 15Q run of pH adjusted homogenate as shown in Figure 17. Lane 1: Mark12 ladder; lane 2: homogenate; lane 3: fraction A1; lane 4: A2; lane 5: A3; lane 6: A4, fractions A1 to A4 correspond to the fractions labeled in Figure 17.

Source 15Q resin has a mean particles size of 15 µm resulting in a higher backpressure compared to resins with larger particles, which could be problematic for the scale up. Therefore, two other strong anion exchange resins were tested: Praesto Q35 jetted with a mean particle size of 35 µm and a Capto Q ImpRes resin with an average particle size of 40 µm.

Moreover, as dilution of the homogenate lead to larger volumes with lower product concentration that had to be purified, a second approach was investigated – buffer exchange of the homogenates by Sephadex G25 prepacked PD10 columns.

The separation of homogenates desalted by buffer exchange to a pH of 8.5 by Capto Q ImpRes and Praesto Q35 jetted resin are illustrated in Figure 19 and Figure 20, respectively. In addition, the salt exchanged homogenate was as well loaded onto the DEAE column but this additional step did not significantly enhance the chromatographic performance of the weak anion exchange resin (data not shown).

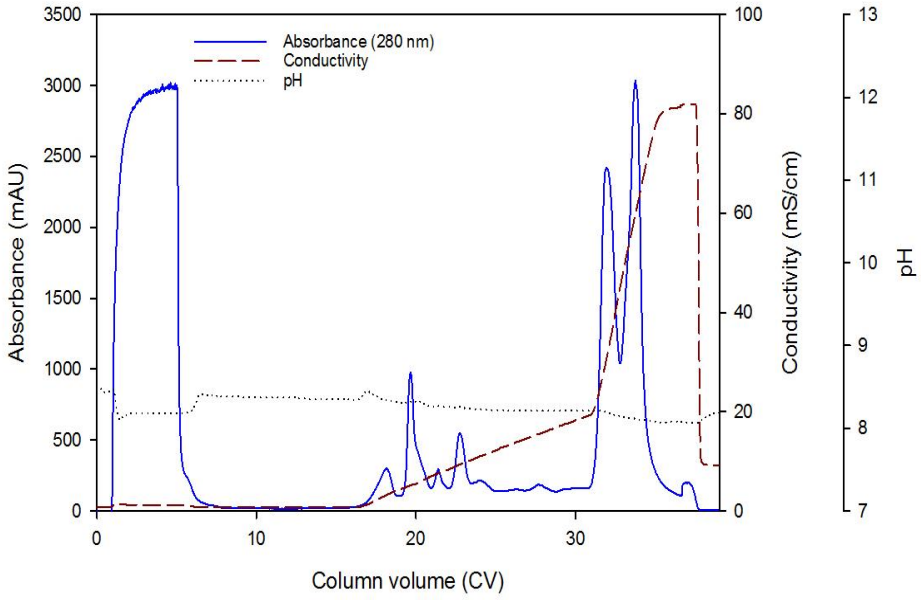

Figure 19: Separation of homogenate desalted to pH 8.5 by Sephadex G25 prepacked columns on Praesto Q35 jetted - 9 mL load; 1 CV = 1.963 mL; TNF-α eluted at conductivity of ~12 mS/cm, which corresponds to 0.12 M NaCl.

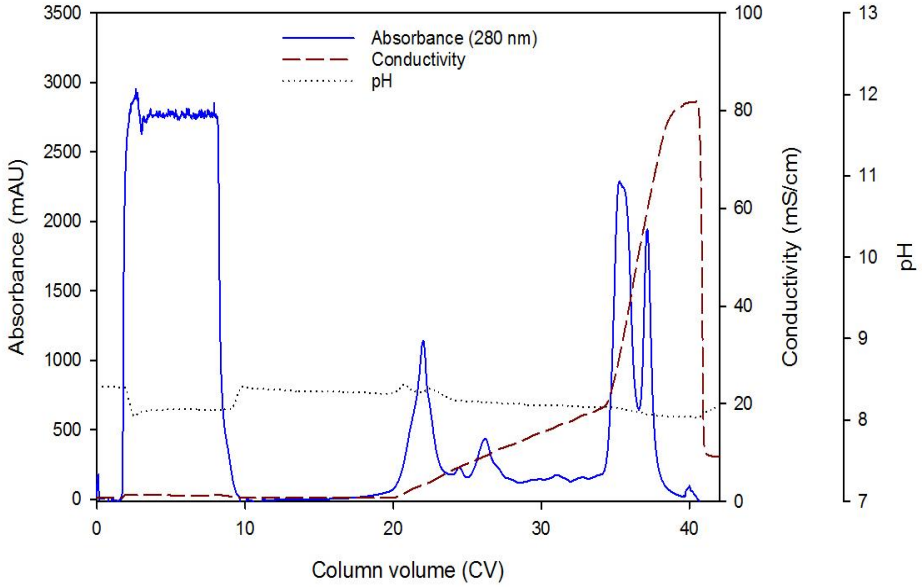

Figure 20: Homogenate desalted via Sephadex G25 in PD10 column to pH 8.5 purified on Capto Q ImpRes - 8 mL load; 1 CV = 1.18 mL; Linear gradient elution with 0-20% buffer B. TNF-α eluted at conductivity of ~5-15-mS/cm.

As the Praesto Q35 showed an adequate performance this resin was used for the first AIEX step in the preparative purification strategy. Furthermore, analytics had shown that the trimeric rh-TNF-α could be found in more than one peak during elution (Figure 18), a step gradient (30% buffer B) was implemented to purify as much protein as possible during the AIEX step. To determine which steps are critical regarding protein loss, a larger volume of 15 mL of the salt exchanged homogenate was loaded onto the Praesto Q35 jetted column (Figure 21).

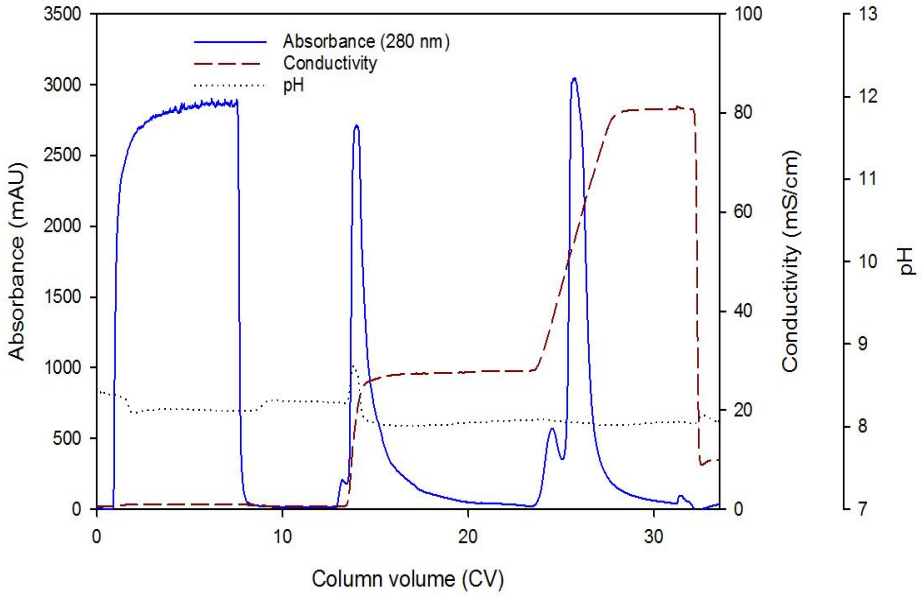

Figure 21: Preparative separation of homogenate desalted pH 8.5 by Sephadex G25 prepacked columns on Praesto Q35 jetted. Load: 15 mL; 1 CV = 2.081 mL; Step gradient elution of 0.3 M NaCl (fraction 1) followed by linear elution step of 0.3 – 1.0 M NaCl (fraction 2).

The first eluate was further purified by a Mono S cation exchange step (Figure 22).

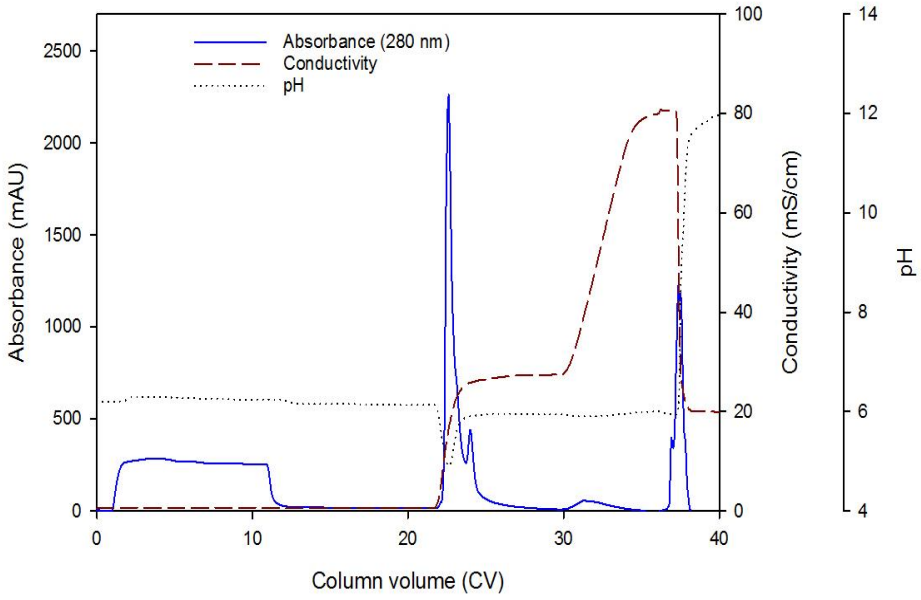

Figure 22: Separation by Mono S cation exchange chromatography of the fraction 1 obtained after preparative purification on Praesto Q35 jetted shown in Figure 21. Load: 10 mL; 1 CV = 0.982 mL; Step gradient of 0.3 M NaCl (fraction 1) followed by linear gradient of 0.3 – 1.0 M NaCl (fraction 2).

The first eluate obtained after separation by Praesto Q35 jetted (Figure 21) and the eluate after separation by the cation exchange resin Mono S (Figure 22) were both analyzed by SEC-HPLC for their content of trimeric TNF-α (Figure 23).

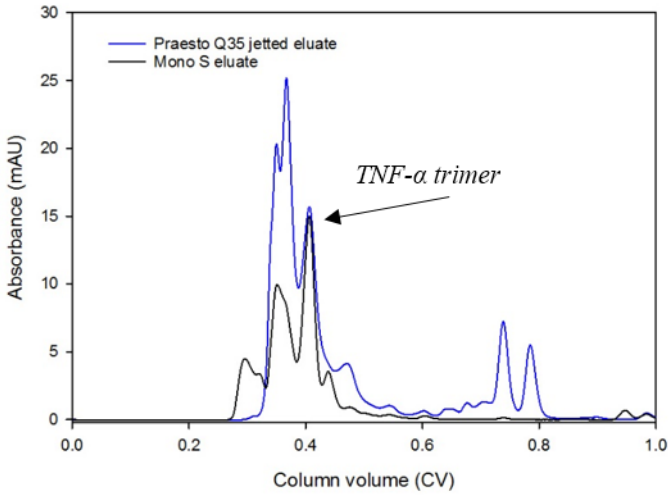

Figure 23: Analytical SEC-HPLC of fraction 1 obtained after separation with Praesto Q35 jetted (solid blue line) and MonoS CIEX first fraction obtained after separation by Mono S (solid black line). Load: 10µL; 1 CV = 23.562 mL. TNF-α retention time at 0.41 CV.

For both purification steps the aliquots of the untreated homogenate, the load, the flow through and the eluates were analyzed by SDS-PAGE (Figure 24). The bands corresponding to a protein with a molecular size of approximately 51 kDa were most likely the trimeric TNF-α. In comparison to the TNF-α standard (Figure 12) other proteins present in the homogenate possibly stabilized the trimeric form to some extent resulting in less reduction of the active TNF-α.

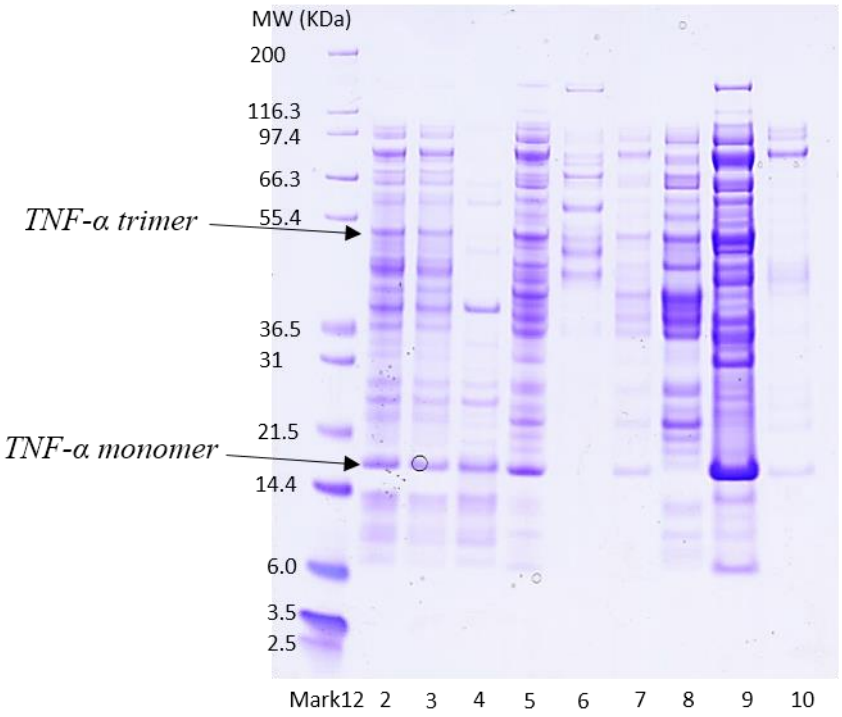

Figure 24: SDS-PAGE of TNF-α preparative purification. Lane 1: Mark12 ladder; 2: Homogenate; 3: salt exchanged homogenate; 4: AIEX flow through; 5: AIEX eluate (fraction 1); 6: AIEX high salt eluate (fraction 2); 7: Salt exchanged AIEX eluate; 8: CIEX flow through; 9: CIEX eluate (fraction 1); 10: CIEX high salt eluate (fraction 2)

Unbound TNF-α monomer was determined in the flow through of the anion exchange step (Figure 24, lane 4).

According to SEC-HPLC (Figure 23) a removal of unwanted components was achieved but analysis by SDS-PAGE showed that the final Mono S CIEX eluate only contained up to 20 % TNF-α trimer (Figure 24, lane 9).

The flow through of the anion exchange separation on the Praesto Q35 jetted was also analyzed by the SEC-HPLC method (Figure 25).

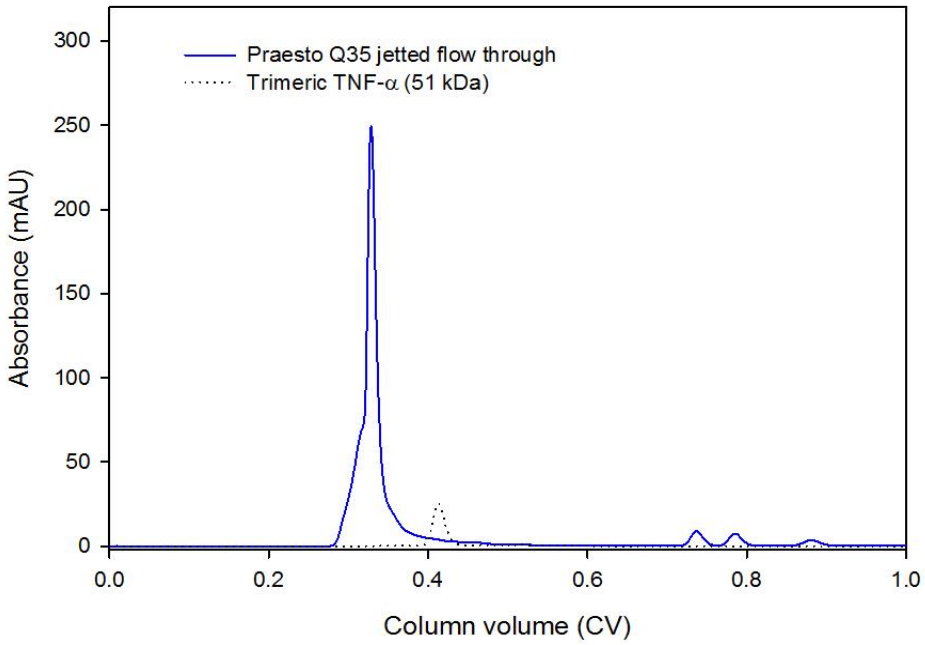

Figure 25: Superdex 75 run of AIEX flow through; Column connected to HPLC device; 10 µL load; 1 CV = 23.562 mL; aggregate retention time of approximately 0.35 CV; TNF-α retention time of ~ 0.41 CV.

In contrast to the analysis by the denaturing SDS-PAGE no monomeric TNF-α was detected by the SEC-HPLC but larger molecules which did not correspond to the TNF-α trimers either but were of larger size in accordance to their smaller retention volume compared to the trimer (Figure 25). TNF-monomers seemed to be bound to other components, resulting in a large heteromeric molecule.

To verify if the aggregates were able to bind adalimumab as the active trimer a dot blot was performed. A series of dilutions of the samples was as well done for visualizing the relation between titer and dye intensity.

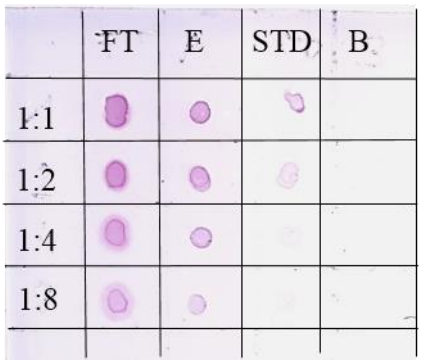

Figure 26: Dot blot of AIEX flow through (FT), eluate (E); TNF-α Standard (STD) and blank (B) (20mM Tris buffer); 1:2 – 1:8 dilutions of samples (diluted with 20 mM Tris buffer);

There was no difference noticeable regarding the binding ability as displayed in Figure 26. Based on this result strategies for the purification and quantification of TNF-α by using antibody-antigen interaction-based methods were not further pursued.

Moreover, by analyzing the Praesto Q35 jetted high salt eluate (fraction 2) fraction by SEC-HPLC a high amount of TNF-α was presumably lost during this step

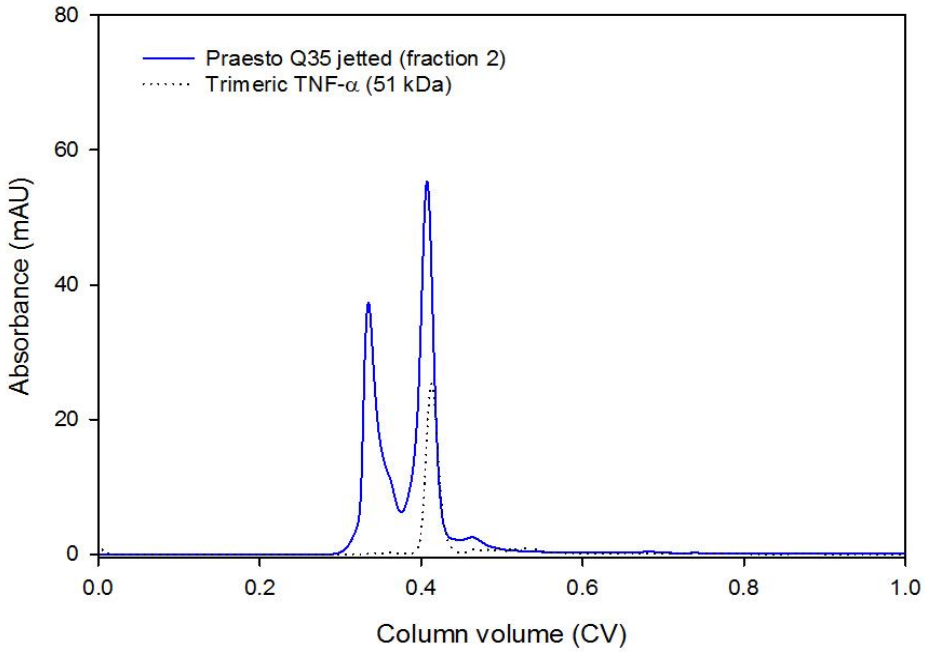

Figure 27: Analytical SEC-HPLC on Superdex 75 of high salt eluate (fraction 2) during separation on Praesto Q35 jetted as shown in Figure 21. Load: 10 µL; 1 CV = 23.562 mL: Identical retention time of unknown protein as trimeric TNF-α (0.41 CV).

Aliquots of this eluate were also analyzed by the analytical AIEX-HPLC on TSK-gel. In contrast to the SEC-analysis, which had indicated the presence of a large amount of TNF-α trimer in this fraction, hardly any trimeric TNF-α was determined by AIEX-HPLC (Figure 28).

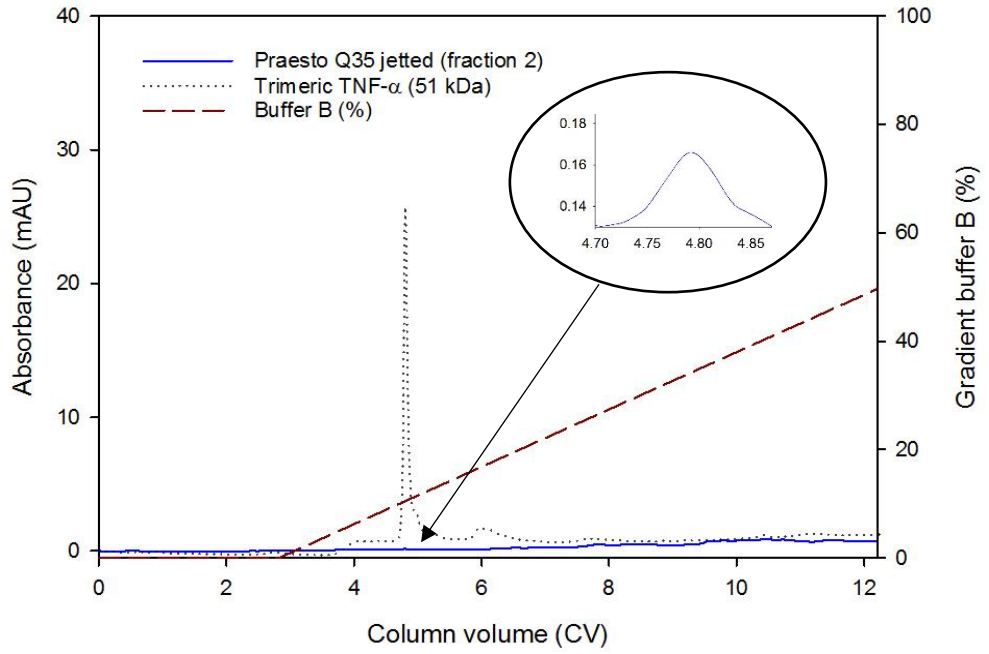

Figure 28: Analytical AIEX-HPLC on TSK-gel of Praesto Q35 jetted high salt eluate (fraction 2). Load: 100 µL; 1 CV= 4.241 mL; linear gradient of 0.0-0.5 M NaCl; enlargement: TNF-α trimer in eluate

In addition, a dot blot was performed (not shown) which showed rarely any adalimumab binding of the components present in this solution.

Summing up these obtained results led to the conclusion that the homogenate additionally contained an unknown component (possibly a protein) that showed similar retentions characteristics, and therefore molecular weight, as TNF-α during SEC analysis by Superdex 75 column but could not be identified by AIEX-HPLC.

The step yields were determined as visible in Table 5. Important to say, two different ways for calculating the step yields were performed:

Due to the presence of the unknown component showing similar molecular size as TNF-α it was impossible to solely quantify the amount of TNF-α in the homogenate using the SEC-HPLC method. Therefore, an assumption was made that all of this component was separated from TNF-α during the first AIEX step. By subtracting the amount of the unknown component in the AIEX high salt eluate from the homogenate, the amount of TNF-α in the starting solution was estimated.

The other way to calculate the step yields was using the analytical AIEX-HPLC method on SAX-gel. Due to a steady drift of the absorbance during the purification of the homogenate on the SAX it was as well just possible to estimate the starting amount of TNF-α

Table 5: Purification steps including calculated protein amount and recovery.

Step	Amount of TNF (mg)		Step yield (%)	
	via SEC	via SAX	via SEC	via SAX
Homogenate (salt exchange)	3.8	2.0	/	
AIEX eluate (Praesto Q35 jetted)	3.4	1.8	~ 90	~90
CIEX start	3.3	1.7	/	/
CIEX eluate (MONO S)	2.2	1.2	~ 65	~70

The most critical step, according to Table 5, regarding loss of TNF-α was the CIEX step. Evaluation and analyzing of the other CIEX fractions (flow through and fraction 2) showed that a large amount of TNF-α was found in the flow through as visible on the SDS-PAGE in Figure 24. Therefore, it was assumed that possibly not all of the TNF-α molecules were charged properly leading in a 30% loss. The difference between both quantification methods was determined as roughly 50%. However, due to many interfering factors it was not possible to establish a highly accurate quantification method.

The overall yield including both chromatographic purification steps was finally determined as ~ 60%.

Due to the presence of unwanted components in the final Mono S eluate a different strategy was chosen for the purpose of achieving high quality. Possible loss of TNF-α during purification steps was accepted. Therefore, an AIEX step gradient run was followed by a CIEX linear gradient. Moreover, the Mono S run is displayed in Figure 29.

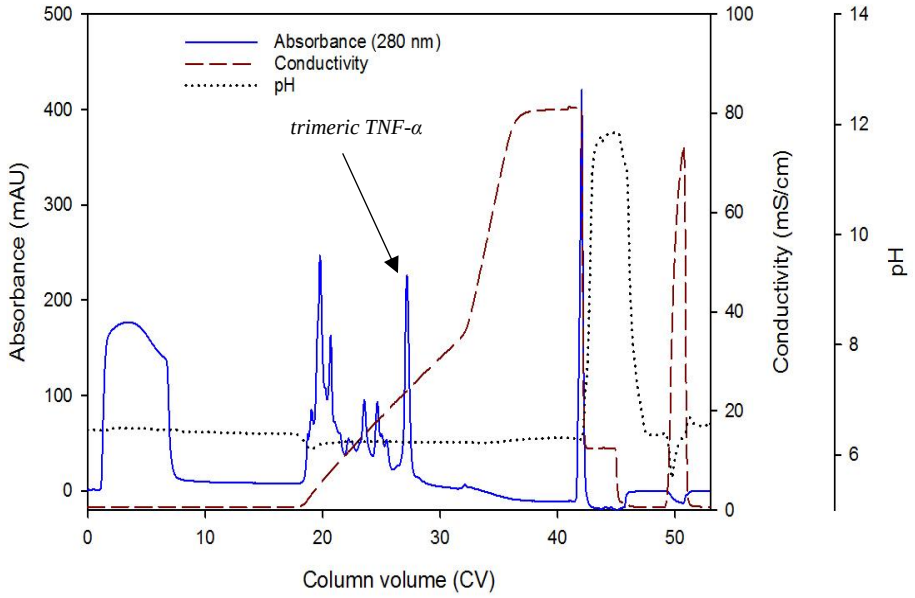

Figure 29: Praesto Q35 jetted eluate purified on Mono S CIEX column. Load: 6 mL; 1 CV = 0.982 mL; Linear gradient 0.0-0.4 M NaCl followed by a 0.4-1.0 M NaCl gradient. Most of TNF-α eluted at 30% buffer B corresponding to a conductivity of 23 mS/cm and 0.3 M NaCl.

As indicated in Figure 29 most of the TNF-α eluted at a buffer B concentration of 0.3 M NaCl. The eluate of the Praesto Q35 jetted run as well as the Mono S fraction containing the protein of interest were further analyzed by SDS-PAGE. As done in other quantification sections, the SEC-HPLC and AIEX-HPLC methods were used for the determination of purity and protein amount.

According to the SDS-PAGE (Figure 30), the Mono S elution fraction containing the active TNF-α trimer was highly pure (Figure 30, lane 4). Moreover, barely any removal of impurities was achieved after the AIEX step carried out by Praesto Q35 jetted (Figure 30, lane 3).

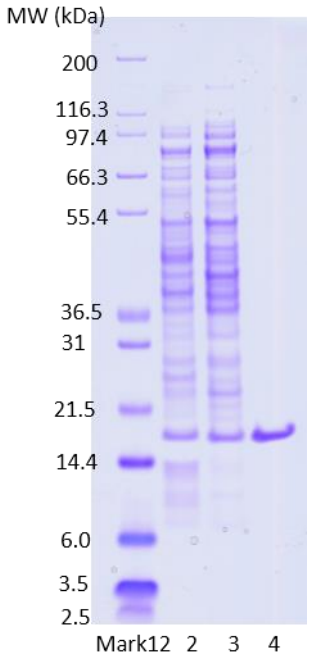

Figure 30: SDS-PAGE of the purification run with linear gradient on the Mono S CIEX column. Well 1: Mark12 ladder; well 2: salt exchanged homogenate; well 3: Praesto Q35 jetted eluate fraction; well 4: Mono S fraction containing highly pure TNF-α

Results obtained by analytical SEC-HPLC (Figure 31) and AIEX-HPLC (Figure 32) confirmed the high purity of the Mono S fraction.

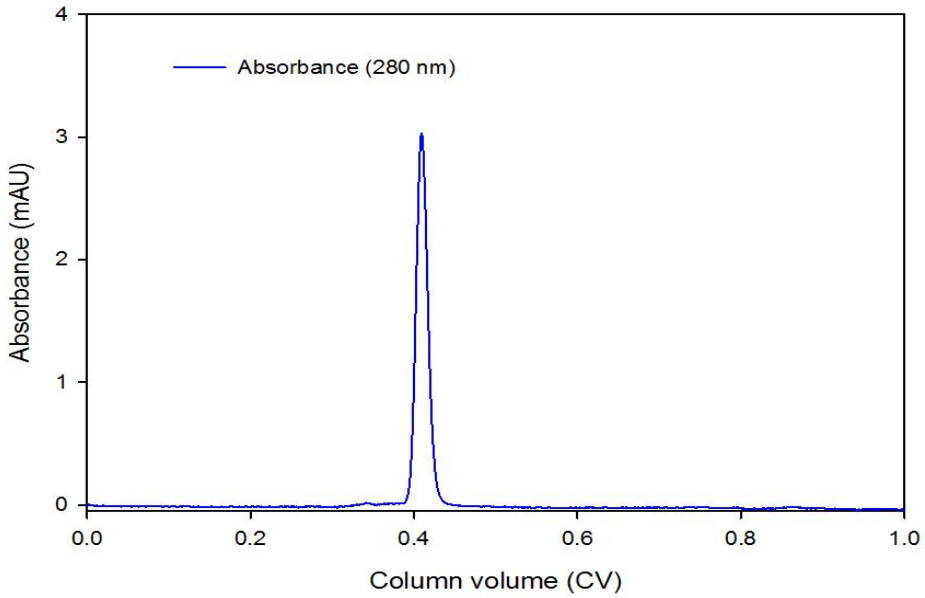

Figure 31: Analytical SEC-HPLC of trimeric fraction of the eluate obtained after separation by Mono S as indicated in Figure 29. Load: 10; 1 CV = 23.562 mL; TNF-α retention time of 0.41 CV.

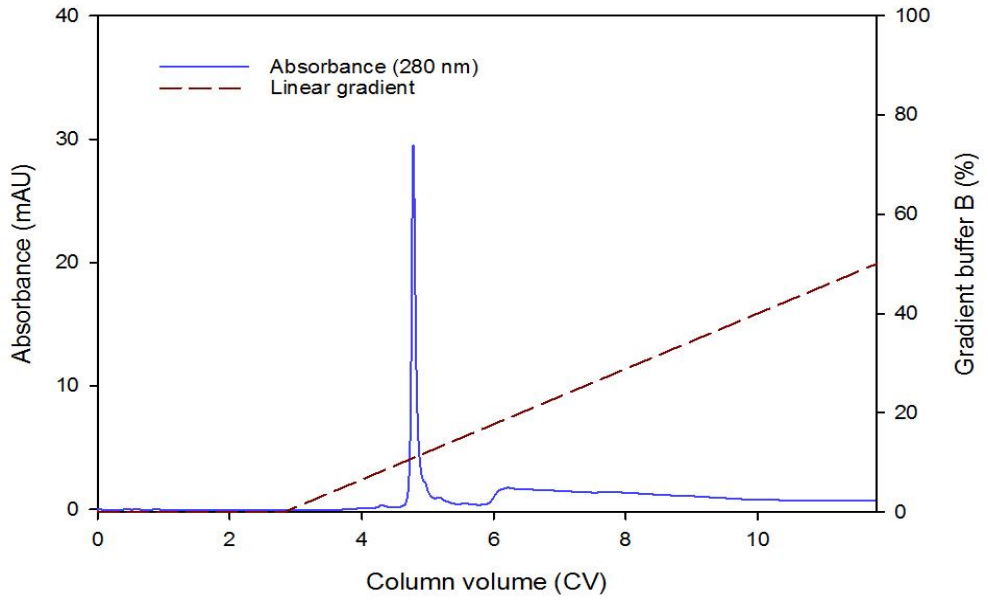

Figure 32: AIEX-HPLC run on TSK-gel SAX of the Mono S fraction containing TNF-α. Load: 100 µL. 1 CV = 4.241 mL; Linear gradient of 0.0-0.5M NaCl. TNF-α eluted at a NaCl concentration of 0.11-0.12 M.

By integrating all present peaks in each chromatogram, the purity of the Mono S fraction was determined. A single TNF-α peak was visible, therefore no other proteins were present. As illustrated in Figure 32 a steady increase of the absorbance is observable during the elution of the TNF-α, which was presumably caused by the increase of salt during elution. This assumption was verified by comparing this section with the TSK-gel SAX chromatogram of the purchased TNF-α standard which should be highly pure (Figure 11).

According to these results the fraction containing rh-TNF-α was highly pure and no other components were present.

In the interest of completeness, the amount of purified TNF-α was as well determined. As described above quantification was performed by applying the AIEX- and the SEC-HPLC method. Both determinations gave equivalent results as shown in Table 6.

Table 6: Quantification of the purified TNF-α by using AIEX-HPLC as well as SEC-HPLC quantification method.

TSK-gel SAX		**Superdex 75 SEC**	
Peak area (mAU*CV)	Calculated amount (µg)	Peak area (mAU*CV)	Calculated amount (µg)
0.063	97.5	2.58	100.2

Moreover, to gain more knowledge about the properties of the aggregates, which had been found in the flow through of the Praesto Q35 jetted step (Figure 24 & Figure 25) additional experiments were performed as discussed in the following section.

3.3. Aggregate characterization

Based on the results of the experiments of chromatographic purification, a detailed study on the characteristics and adsorption behavior of the aggregates was performed.

3.3.1. Identification of the aggregate forming components

For the identification of the individual components that had formed the heteropolymeric aggregates, which already had been analyzed on the SEC-HPLC column (Figure 25) an external peptide mapping was performed in the department of chemistry. Prior to the mapping a SDS-PAGE was performed. By purifying the flow through of the AIEX run on the size exclusion column and further loading the fraction of interest several times on the SDS-PAGE a separation of the aggregate was achieved. Three bands on the gel, which were obviously one of the major components responsible for the heteropolymer formation were cut out of the gel, enzymatically processed and further analyzed via QTOF ESI MS. Figure 33 shows the three marked bands (A,B,C) of interest.

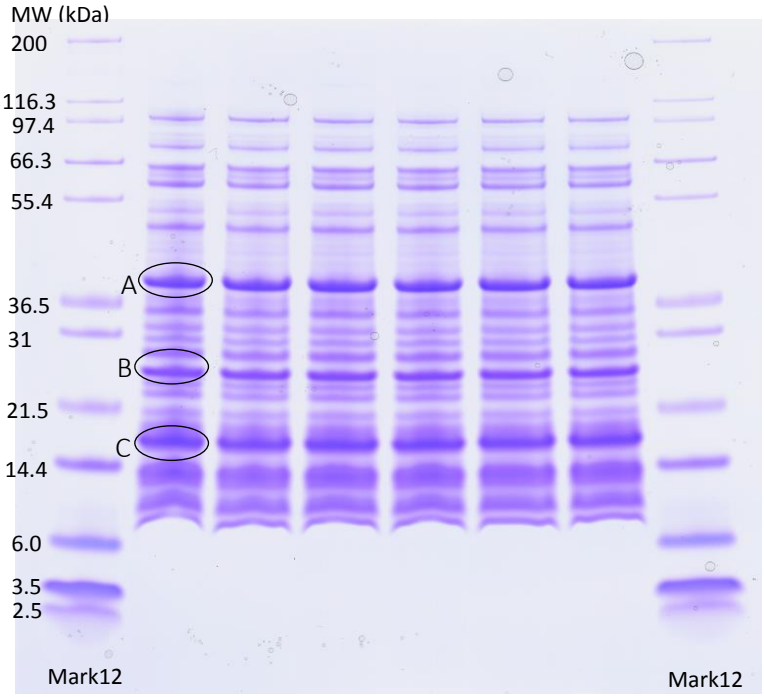

Figure 33: SDS-PAGE of the flow through for peptide mapping; Mark12 standard used as reference molecules with known molecular weights.

The peptide sequence analysis suggested that band **A** is the outer membrane protein F (ompF) of the E. coli strain K12 (sequence coverage: 72.7 % and MASCOT score: 1201.5). This outer membrane protein is a 40-kDa large protein located, as the name implies, on the outer membrane of E. coli responsible for immune response as well as enabling passive diffusion [46]. Based on the sequence analysis, Band **B** represents the phage shock protein A of strain K12 (sequence coverage: 75.7 % and MASCOT score: 958.8). Phage shock protein A is a 26 kDa large protein which is as well bound peripherally to the inner membrane [47]. According to Uniprot [48] there is a high homology between strain BL21 and strain K12. The major difference between these strains is the absence of genes including the flagellar component gene, ompT and a DNA cytosine methylase dcm in BL21. Finally, band **C** represents the TNF-α monomer (17.4 kDa protein) as expected (sequence coverage: 61.6 % and MASCOT score: 611.3).

Summing up, the major components responsible for the formation of the polymeric aggregates are according to peptide mapping investigations outer membrane protein F, phage shock protein A as well as monomers of TNF-α.

3.3.2. Urea and heat stability of aggregates

Investigations were performed to evaluate if the aggregates can be eliminated in a single step. This was done on the one hand by mixing the flow through of the homogenate with different urea concentrations and on the other hand by treating the homogenate with heat.

As explained in the method section, the Praesto Q35 jetted flow through containing the aggregates was treated with a series of Urea concentrations. Decrease of the Praesto flow through was measured by SEC-HPLC analysis. The decline of the amount of aggregates is displayed in Figure 34.

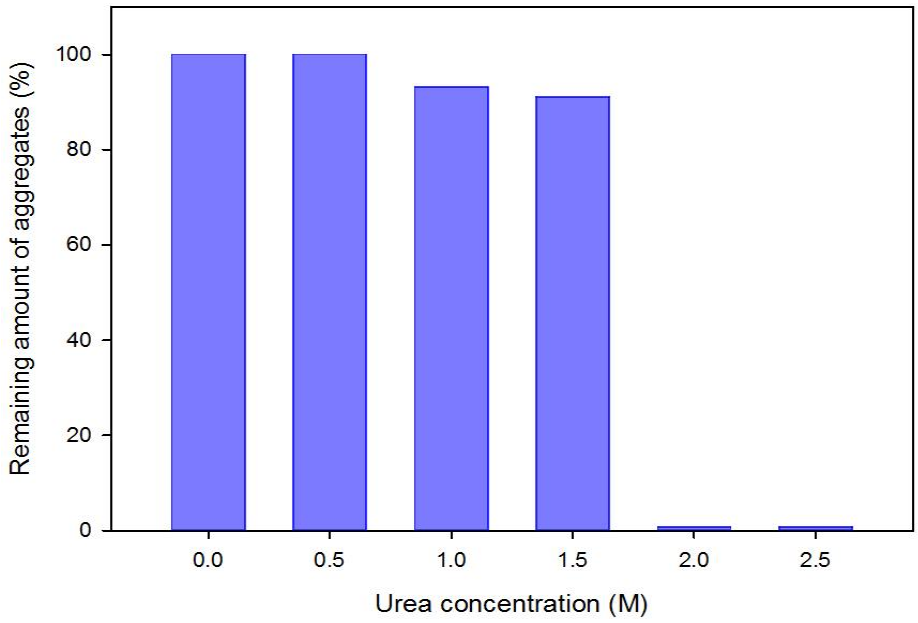

Figure 34: Denaturation of aggregates with various urea concentrations; Urea concentration corresponds to the final concentration of urea in the reaction tubes.

A minimum concentration of 2.0 M urea was necessary for disassembling of the aggregates (Figure 34). In addition, 2.5 urea led to similar results as illustrated in Figure 35.

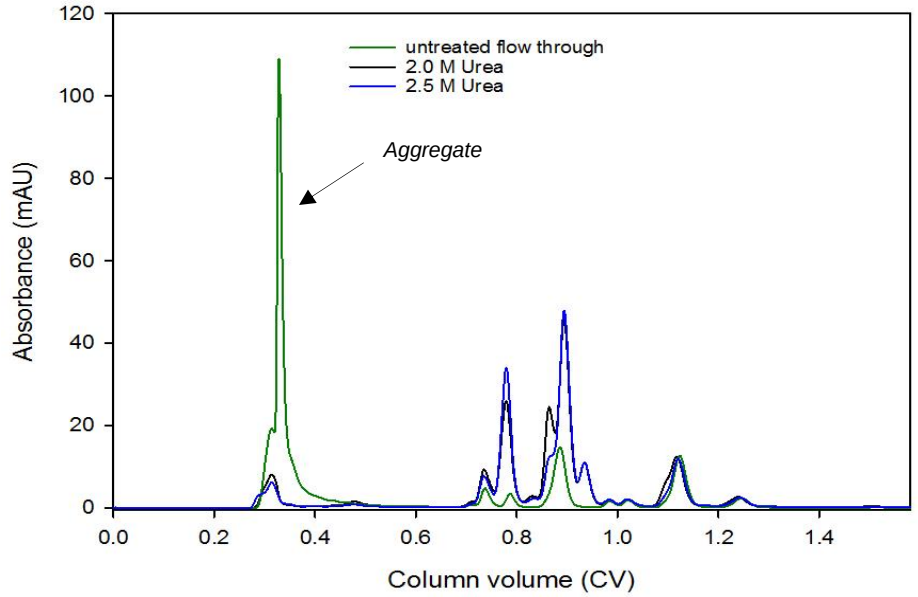

Figure 35: Overlay of urea treatment runs of flow through; Superdex 75 connected to HPLC device; 10 µL load; 1 CV = 23.562 mL; Peak at retention time of ~ 0.35 CV indicates the present aggregates.

In contrast to the aggregates, TNF-α trimers in the AIEX eluates were stable upon 2.0 M Urea treatment as shown in Figure 36. This would possibly enable a wash step prior to purification for removing interfering aggregates.

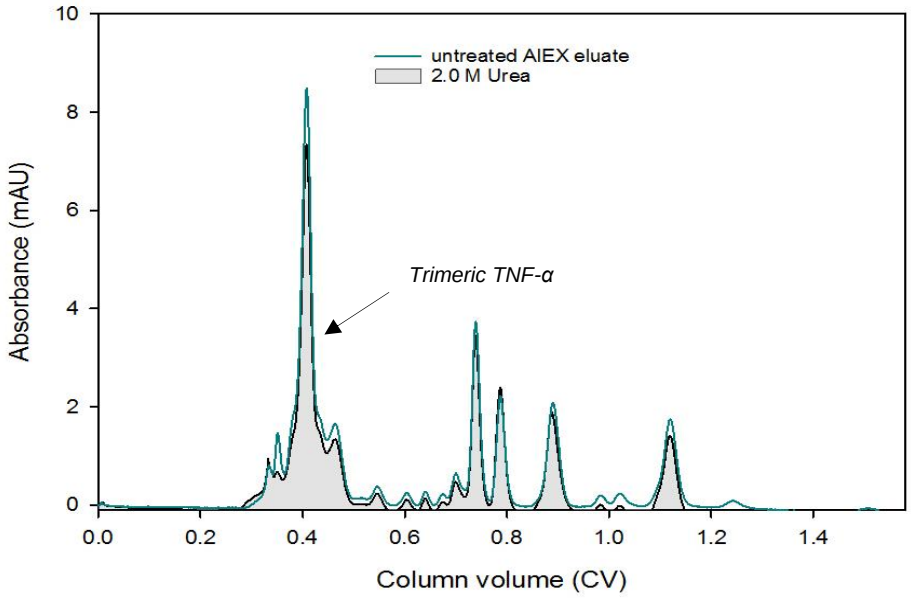

Figure 36: 2.0 M Urea treatment of AIEX eluate; Superdex 75 connected to HPLC device; 10 µL load; 1 CV = 23.562 mL; Hardly any reduction of TNF-α (retention time of ~0.41 CV) as indicated in the grey filled curve.

By applying different heat conditions, the stability of the aggregates as well as of TNF-α trimer were determined. As done for the urea stability trial, the untreated homogenate was measured as well to obtain a reference value. Both components were stable/instable at the same temperature conditions in a similar manner. The progresses of the decrease of the aggregate and the TNF-α are displayed in (Figure 37).

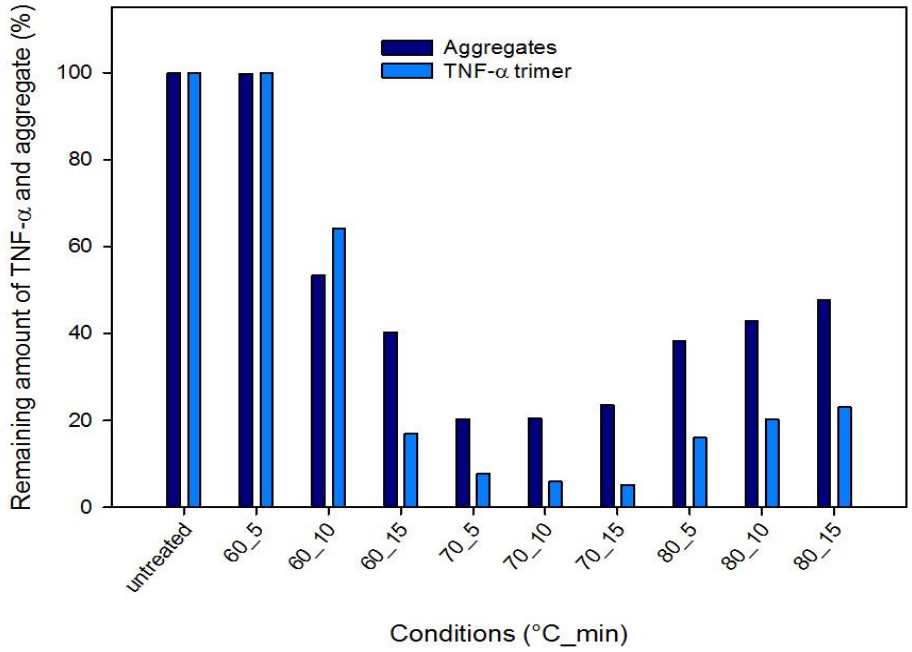

Figure 37: Heat precipitation of homogenate - stability of aggregates and TNF-α trimer; Decrease of the amount of aggregates/TNF-α from 60 °C for 10 min to 70° C for 15 min; Slight increase of the amount at higher temperature;

Interestingly, an increase of the amount in both components at 80 °C with increasing treatment time was observed. This could be explained by a rise of solubility at higher temperatures or simply inaccuracy of the measurement method.

According to these results, this method is less adequate for disassembling of the aggregates due to similar heat stability properties of TNF-a trimers. The most suitable result was obtained by treating the homogenate with 60°C for 10 minutes. Thereby, a decrease of the aggregate of approximately 50% was achieved. However, this led as well to a titer reduction of the TNF-α of roughly 40%.

Presumably, applying of lower temperatures for a distinct time could overcome this issue.

3.3.3. Aggregate binding behavior - loading larger amounts of homogenate

To further investigate if the aggregates were always unable to bind to the Praesto Q35 resin, different volumes of the homogenate were loaded onto the AIEX resin (Figure 38). 10-38 mL sample volume were applied which corresponded to 2-7.5 mg trimeric TNF-α.

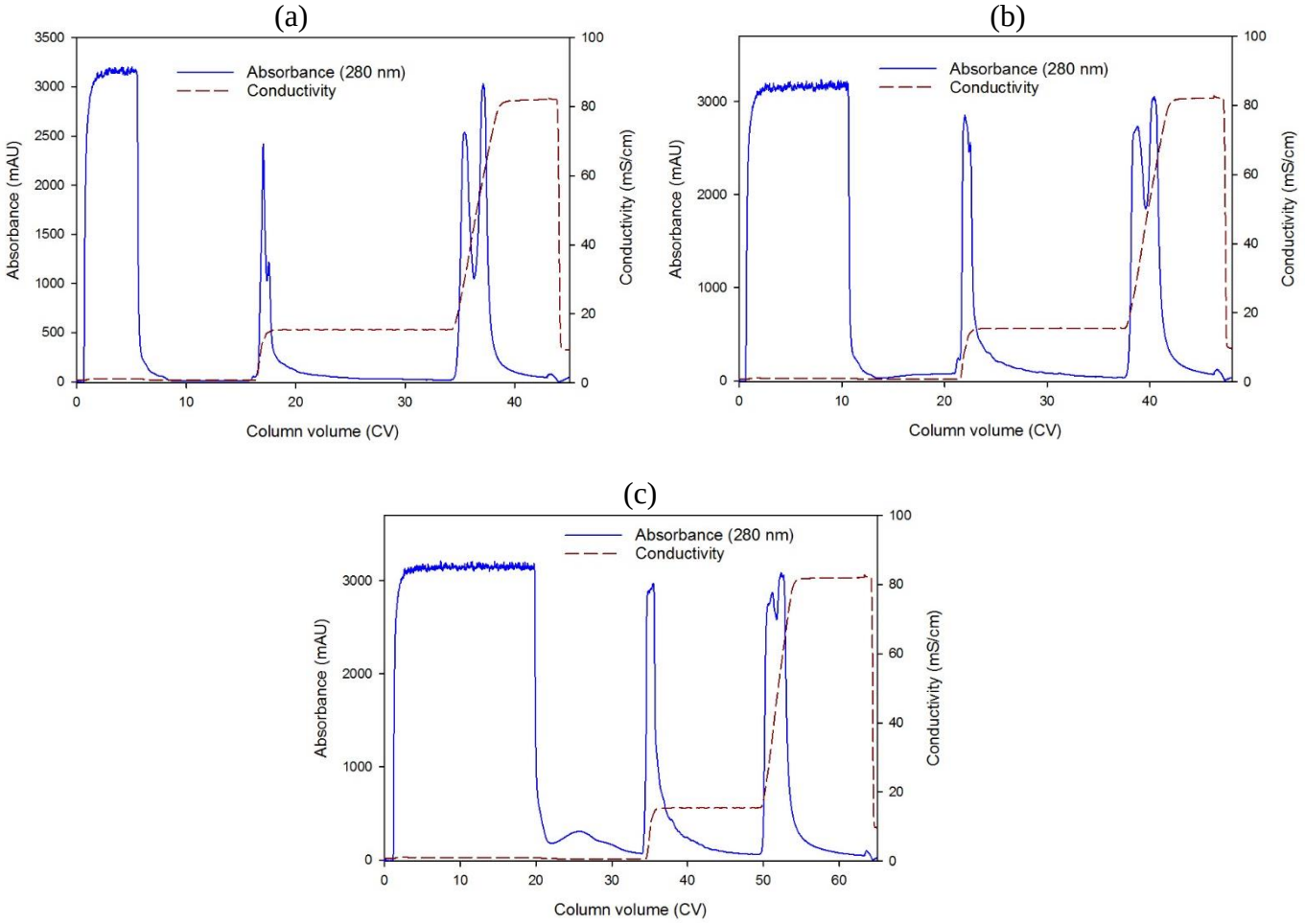

Figure 38: Different volumes of salt exchanged homogenate loaded onto Praesto Q35 jetted. 1 CV = 1.963 mL; Step gradient 0.0-0.2 M NaCl followed by linear gradient of 0.2-1.0 M; Figure (a): 10 mL load of desalted homogenate; (b): 20 mL load of desalted homogenate; (c): 38 mL load of desalted homogenate;

All eluates were analyzed by using the SEC-HPLC method on Superdex 75 (Figure 39).

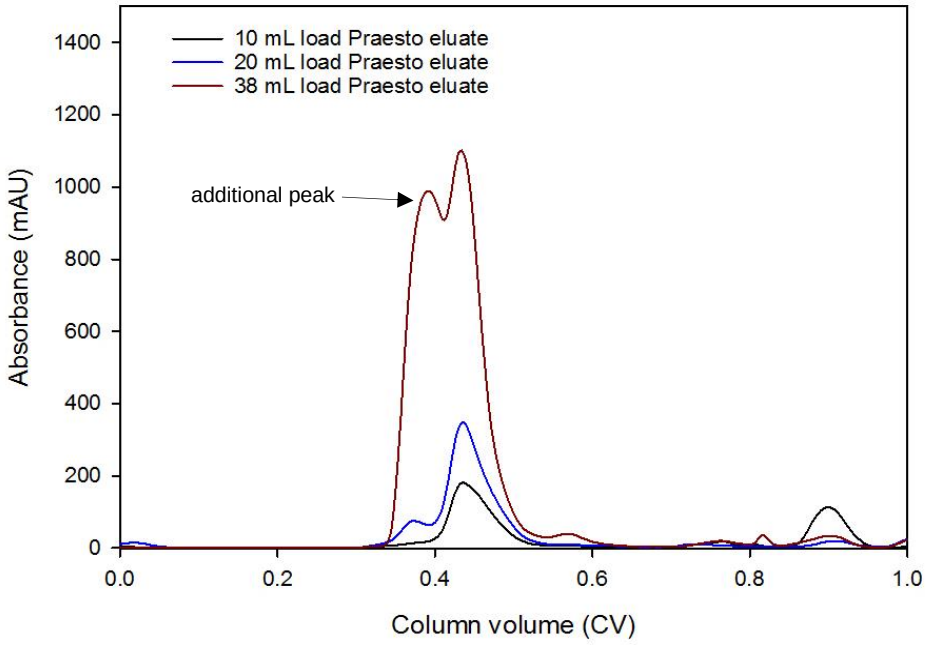

Figure 39: Overlay of Praesto Q35 jetted eluates analyzed via SEC-HPLC method on Superdex 75. Load: 200 µL; 1 CV = 23.562 mL; additional peak at retention time of ~0.39 CV at higher loading of homogenate onto Praesto Q35 jetted.

The overlay of the SEC-HPLC runs shows an increase of an additional peak at a retention of approximately 0.39 column volumes. Both peaks of the 38 mL load SEC runs were further analyzed by SDS-PAGE visualized in Figure 40.

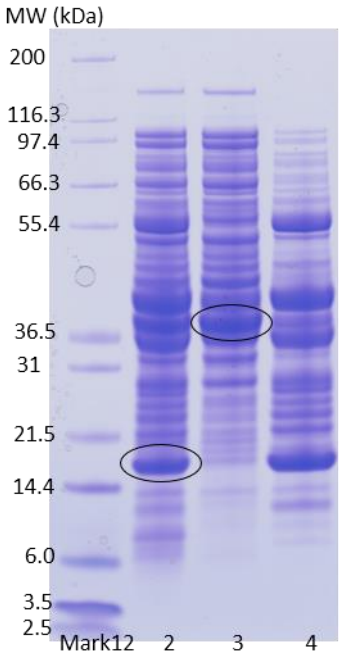

Figure 40: SDS-PAGE of 38 mL eluate and eluate further purified by SEC-HPLC on Superdex 75; Lane 1: Mark12 ladder; lane 2: Praesto Q35 jetted eluate; lane 3: additional peak of SEC run; lane 4: SEC peak at TNF-α retention time (~0.41 CV).

Lane 3, which corresponds to the additional peak, showed hardly any TNF-α bands. The major component was a protein with a molecular weight of approximately 40 kDa. As described in the section this band could possibly be the outer membrane protein F which was present in the flow through in large amounts.

Therefore, a higher loading volume resulted in an enrichment of components, which were basically responsible for aggregate formation. This could complicate further purification steps.
Moreover, an additional CIEX step gradient did not enable separation of the entrained components from TNF-α (data not shown).

Finally, to rule out that the aggregates resulted from the contact time with the chromatographic resins an AIEX run was performed with 2% PEG200 added in the desalting buffer for stabilization of the protein. The comparison of both analytical SEC runs (with and without PEG200) is displayed in Figure 41. No difference was observed in the peak profile and therefore, the titer of TNF-α was as well not increased.

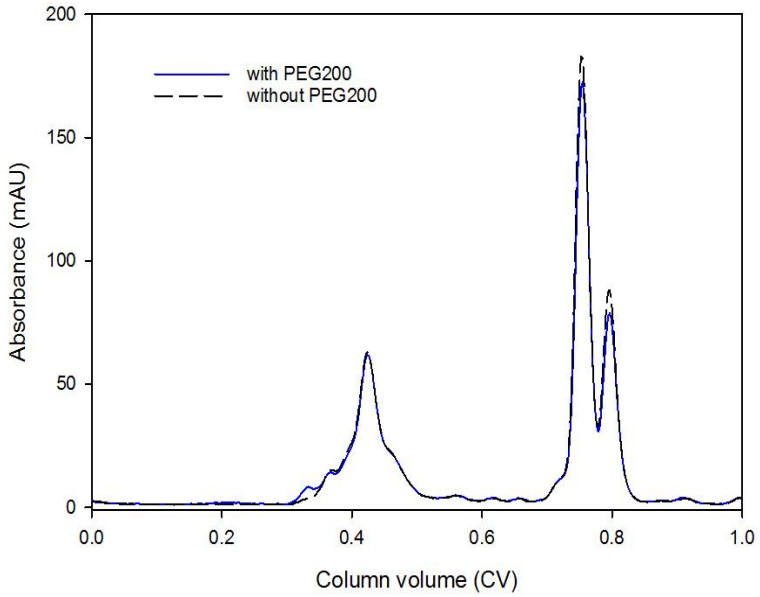

Figure 41: Comparison of Superdex 75 runs of Praesto Q35 eluates with and without PEG addition – 200 µL load; 1 CV = 23.562 mL;

4. Conclusion and Outlook

The initial goal of this, the establishment of a purification process for obtaining active TNF-α, was partly accomplished. A two-stage chromatographic process based on an anion exchange chromatography step followed by a cation-exchanger step was developed. Elution of proteins was performed by using a step gradient with NaCl for both IEX steps. This led to an overall process yield of approximately 60% of trimeric TNF-α under optimized condition. Analysis of the final composition revealed a rather low purity of only 20%. Therefore, a linear NaCl gradient was implemented for the cation exchange chromatography step. This modified strategy enabled purification of active TNF-α with high purity (> 95%). Further analysis and quantification showed that a lot of the trimer was lost during the CIEX step leading to an overall yield of approximately 5%. The reason for the high loss was the fact that the major fraction of the active cytokine eluted in association with *E.coli* host cell proteins. In addition, low binding capacity of the cation exchange steps was another crucial limitation regarding the purification process.

Furthermore, intensive studies on the composition of the primary cell homogenate revealed that the majority of the produced TNF-α was bound to other host cell components resulting in formation of large aggregates. Sequence analysis showed that beside monomeric units of TNF-α, the outer membrane protein F as well as the phage shock protein A were major components responsible for aggregate formation. The cause for the formation and origin of the aggregates could not been determined. Further experiments led to the result that the reduced binding capacity of the trimeric TNF-α on the IEX resins was as well affected by the presence of the polymeric aggregates.

Studies on the stability of the aggregates revealed that the presence of 2 M urea resulted in a complete destabilization of the aggregates. Based on this outcome an additional urea wash step could overcome the interfering effect of the aggregates especially regarding binding capacity on ion exchangers. Furthermore, heat stability experiments showed that by applying a temperature of 60°C for 10 minutes disassembling of the present aggregates of approximately 60% could be achieved. Therefore, implementation of a heat precipitation step could possibly as well improve further purification steps. Nevertheless, additional studies on the cause and origin of the aggregate formation should be performed to possibly create the base for new strategies for the purification of highly pure TNF-α in large amounts.

In summary, a two-stage chromatographic process has been established to yield highly pure TNF-α. Also, in-depth process understanding was gained which is required for optimizing of TNF-α production including improvement of primary recovery and conditioning of the cell homogenate.

Abbreviation

AIEX	*Anion exchange chromatography*
Ala76	*Alanine residue at position 76*
BSA	*Bovine serum albumin*
CIEX	*Cation exchange chromatography*
Cys	*Cysteine*
DEAE	*Diethylaminoethanol*
ESI	*Electrospray ionization*
E. coli	*Escherichia coli*
FT	*Flow through*
HPLC	*High performance liquid chromatography*
HQ	*High quality*
IB	*Inclusion body*
IEX	*Ion exchange chromatography*
IgG	*Immunoglobulin G*
LC	*Liquid chromatography*
mAb	*Monoclonal antibody*
MS	*Mass spectrometry*
pI	*Isoelectric point*
omp	*Outer membrane protein*
PEG	*Polyethylene glycol*
QTOF	*Quadrupole time-of-flight*
RO	*Reverse osmosis*
TNF	*Tumor necrosis factor*
rh-TNF-α	*Recombinant human TNF-α*
SAX	*Strong anion exchange*
SDS-PAGE	*Sodium dodecyl sulfate polyacrylamide gel electrophoresis*
sTNF- α	*Soluble TNF- α*
tmTNF- α	*Transmembrane TNF-α*
TNFR	*Tumor necrosis factor receptor*
TACE	*Tumor necrosis factor-α converting enzyme*
Val77	*Valine residue at position 77*

I. List of Figures

II. List of Tables

III. List of Reference

1. Ramadan, H. A. I., Saini, K. S., Baeshen, N. A. & Redwan, E. M. Journal.Pone.0190925.S005. **25**, 953–962 (2015).
2. van Bloois, E. Biotechnological applications of periplasmic expression in E. coli. *Enzym. Eng.* **1**, 2–4 (2013).
3. Rosano, G. L. & Ceccarelli, E. A. Recombinant protein expression in Escherichia coli: Advances and challenges. *Front. Microbiol.* **5**, 1–17 (2014).
4. Schumann, W. & Ferreira, L. C. S. Production of recombinant proteins in Escherichia coli. *Genet. Mol. Biol.* **27**, 442–453 (2004).
5. Zhang, J.-M. & An, J. Cytokines, Inflammation, Pain. *Int Anesth. Clin.* **69**, 482–489 (2009).
6. Kupsa, T., Horacek, J. M. & Jebavy, L. The role of cytokines in acute myeloid leukemia: A systematic review. *Biomed. Pap.* **156**, 291–301 (2012).
7. Zon, M. J.-B. and L. I. Hematopoiesis. *Brenner's Encycl. Genet. Second Ed.* **2467**, 418–421 (2013).
8. Chamoto, K., Al-Habsi, M. & Honjo, T. Current Topics in Microbiology and Immunology: Role of PD-1 in Immunity and Diseases. *Springer Int. Publ.* **410**, 75–97 (2017).
9. Wang, X. & Lin, Y. Tumor necrosis factor and cancer, buddies or foes? *Acta Pharmacol. Sin.* **29**, 1275–1288 (2008).
10. Benveniste, E. N. Cytokines. *Encycl. Neurol. Sci.* **2**, 921–925 (2014).
11. Aggarwal, B. B., Gupta, S. C. & Kim, J. H. Historical perspectives on tumor necrosis factor and its superfamily: 25 years later, a golden journey. *Blood* **119**, 651–665 (2012).
12. Beutler, B. *et al.* Identity of tumour necrosis factor and the macrophage-secreted factor cachectin. *Nature* **316**, 552–554 (1985).
13. Tang, P., Hung, M. C. & Klostergaard, J. Human pro-tumor necrosis factor is a homotrimer. *Biochemistry* **35**, 8216–8225 (1996).
14. Horiuchi, T., Mitoma, H., Harashima, S. I., Tsukamoto, H. & Shimoda, T. Transmembrane TNF-α: Structure, function and interaction with anti-TNF agents. *Rheumatology* **49**, 1215–1228 (2010).
15. Mohan, M. J. *et al.* The tumor necrosis factor-α converting enzyme (TACE): A unique metalloproteinase with highly defined substrate selectivity. *Biochemistry* **41**, 9462–9469 (2002).
16. Abel Lajtha. Handbook of Neurochemistry and Molecular Neurobiology - Neuroactive Proteins and Peptides. **3rd Editio**, 179 (2006).
17. RCSB Protein Data Bank. Available at: https://www.rcsb.org/pdb/explore/remediatedSequence.do?structureId=1TNF&

params.chainEntityStrategyStr=all&forcePageForChain=B. (Accessed: 10th April 2019)

18. JONES, E. Y., STUART, D. I. & WALKER, N. P. C. The structure of tumour necrosis factor - implications for biological function. *J. Cell Sci.* **1990**, 11–18 (2013).

19. Kiraga, J. *et al.* The relationships between the isoelectric point and: Length of proteins, taxonomy and ecology of organisms. *BMC Genomics* **8**, 1–16 (2007).

20. Zhang, C. *et al.* Facile purification of Escherichia coli expressed tag-free recombinant human tumor necrosis factor alpha from supernatant. *PROTEIN Expr. Purif.* **95**, 195–203 (2014).

21. Novák, P. & Havlíček, V. Protein Extraction and Precipitation. *Proteomic Profiling Anal. Chem. Crossroads Second Ed.* 52–62 (2016). doi:10.1016/B978-0-444-63688-1.00004-5

22. Panicker, G., Meadows, K. S., Lee, D. R., Nisenbaum, R. & Unger, E. R. Effect of storage temperatures on the stability of cytokines in cervical mucous. *Cytokine* **37**, 176–179 (2007).

23. Aziz, N. *et al.* Stability of cytokines, chemokines and soluble activation markers in unprocessed blood stored under different conditions. *Cytokine* **84**, 17–24 (2016).

24. Biesmans, S. *et al.* Peripheral Administration of Tumor Necrosis Factor-Alpha Induces Neuroinflammation and Sickness but Not Depressive-Like Behavior in Mice. *Biomed Res. Int.* **2015**, 1–14 (2015).

25. Zelová, H. & Hošek, J. TNF-α signalling and inflammation: Interactions between old acquaintances. *Inflamm. Res.* **62**, 641–651 (2013).

26. Tian, T., Wang, M. & Ma, D. TNF- α , a good or bad factor in hematological diseases? 31. 1–12 (2014). doi:10.3978/j.issn.2306-9759.2014.04.02

27. Cai, W., Kerner, Z. J., Hong, H. & Sun, J. Targeted Cancer Therapy with Tumor Necrosis Factor-Alpha. *Biochem. Insights* **1**, BCI.S901 (2017).

28. Novacek, G. *et al.* Adalimumab for the treatment of adult Crohn's disease--update of a consensus report by the Working Group Inflammatory Bowel Disease of the Austrian Society of Gastroenterology and Hepatology. *Adalimumab der Behandlung des adulten Morb. Crohn--Update eines Konsensus der Arbeitsgr. Chron. Entzundliche Darmerkrankungen der Osterr. Gesellschaft fur Gastroenterol. und Hepatol.* **51**, 1101–1109 (2013).

29. Curnis, F. & Corti, A. Production and Characterization of Recombinant Human and Murine TNF. **98**,

30. Hoffmann, A. *et al.* Recombinant production of bioactive human TNF- a by SUMO-fusion system – High yields from shake-flask culture. *Protein Expr. Purif.* **72**, 238–243 (2010).

31. Singh, A., Upadhyay, V., Upadhyay, A. K., Singh, S. M. & Panda, A. K. Protein recovery from inclusion bodies of Escherichia coli using mild solubilization process. *Microb. Cell Fact.* **14**, 1–10 (2015).

32. Wang, Y. *et al.* One-step refolding and puri fi cation of recombinant human tumor necrosis factor- α (rhTNF- α) using ion-exchange chromatography. 305–311 (2015). doi:10.1002/bmc.3276

33. Doran, P. M. Unit Operations - Bioprocess Engineering Principles, Second Edition. *Handb. Pap. Board Second Ed.* **1**, 351–472 (2013).

34. Stephen Olaribigbe Majekodunmi. A Review on Centrifugation in the Pharmaceutical Industry. *Am. J. Biomed. Eng.* **5**, 67–78 (2015).

35. R. Ahmad-Raus, M. Mel, S. N. M.-A. and K. Y. Cell Rupture of Recombinant Escherichia coli using High Pressure Homogenizer. **9**, 11–22

36. Dhankhar, P. Homogenization Fundamentals. *IOSR J. Eng.* **4**, 01–08 (2014).

37. Hahn, R. Methods for characterization of biochromatography media. *J. Sep. Sci.* (2012). doi:10.1002/jssc.201200770

38. Carta, G. & Jungbauer, A. *Protein Chromatography*. *Protein Chromatography* (2010). doi:10.1002/9783527630158

39. I, M. C. B. *et al.* A study of interleukin 6 (IL-6) and tumor necrosis factor alpha (TNF-α) serum levels in rats subjected to fecal peritonitis and treated with intraperitoneal ropivacaine. **27**, 494–498

40. Camper, D. M. V. & Viola, R. E. Fully automated protein purification. *Anal. Biochem.* **393**, 176–181 (2009).

41. Meyerhoff, G. Application of gel chromatography. *Pure Appl. Chem.* **20**, 309–327 (2008).

42. Bird, I. M. High performance liquid chromatography: principles and clinical applications. *Bmj* **299**, 783–787 (2009).

43. Malviya R, Bansal V, P. O. P. and S. P. K. High performance liquid chromatography: a short review. *J. Glob. Pharma Technol.* **2**, 22–26 (2010).

44. Manns, J. M. SDS-polyacrylamide gel electrophoresis (SDS-PAGE) of proteins. *Curr. Protoc. Microbiol.* 1–13 (2011). doi:10.1002/9780471729259.mca03ms22

45. Poxton, I. R. lmmunoblotting techniques. 905–909 (1990).

46. Wang, X. *et al.* Escherichia coli outer membrane protein F (OmpF): an immunogenic protein induces cross-reactive antibodies against Escherichia coli and Shigella. *AMB Express* **7**, (2017).

47. Adams, H., Teertstra, W., Demmers, J., Boesten, R. & Tommassen, J. Interactions between phage-shock proteins in Escherichia coli. *J. Bacteriol.* **185**, 1174–1180 (2003).

48. Uniprot. Available at: https://www.uniprot.org/proteomes/UP000001509. (Accessed: 18th April 2019)